Canadian Experiment for Soil Moisture in 2010 (CanEx-SM10): Overview and Preliminary Results

Ramata Magagi, *Member, IEEE*, Aaron A. Berg, Kalifa Goïta, *Member, IEEE*, Stephane Bélair, Thomas J. Jackson, *Fellow, IEEE*, Brenda Toth, Anne Walker, Heather McNairn, Peggy E. O'Neill, *Senior Member, IEEE*, Mahta Moghaddam, *Fellow, IEEE*, Imen Gherboudj, *Associate Member, IEEE*, Andreas Colliander, *Senior Member, IEEE*, Michael H. Cosh, Mariko Burgin, *Student Member, IEEE*, Joshua B. Fisher, Seung-Bum Kim, Iliana Mladenova, *Member, IEEE*, Najib Djamaï, Louis-Philippe B. Rousseau, Jon Belanger, Jiali Shang, *Member, IEEE*, and Amine Merzouki

***Abstract*—The Canadian Experiment for Soil Moisture in 2010 (CanEx-SM10) was carried out in Saskatchewan, Canada, from 31 May to 16 June, 2010. Its main objective was to contribute to Soil Moisture and Ocean Salinity (SMOS) mission validation and the prelaunch assessment of the proposed Soil Moisture Active and Passive (SMAP) mission. During CanEx-SM10, SMOS data as well as other passive and active microwave measurements were collected by both airborne and satellite platforms. Ground-based measurements of soil (moisture, temperature, roughness, bulk density) and vegetation characteristics (leaf area index, biomass, vegetation height) were conducted close in time to the airborne and satellite acquisitions. Moreover, two ground-based *in situ* networks provided continuous measurements of meteorological conditions and soil moisture and soil temperature profiles. Two sites, each covering 33 km $\times$ 71 km (about two SMOS pixels) were selected in agricultural and boreal forested areas in order to provide contrasting soil and vegetation conditions. This paper describes the measurement strategy, provides an overview of the data sets, and presents preliminary results. Over the agricultural area, the airborne L-band brightness temperatures matched up well with the SMOS data (prototype 346). The radio frequency interference observed in both SMOS and the airborne L-band radiometer data exhibited spatial and temporal variability and polarization dependency. The temporal evolution of the SMOS soil moisture product (prototype 307) matched that observed with the ground data, but the absolute soil moisture estimates did not meet the accuracy requirements (0.04 $\mathrm{m}^3/\mathrm{m}^3$) of the SMOS mission. AMSR-E soil moisture estimates from the National Snow and Ice Data Center more closely reflected soil moisture measurements.**

***Index Terms*—Agricultural and boreal forested areas, brightness temperature, soil moisture, Soil Moisture and Ocean Salinity (SMOS), validation.**

Manuscript received April 8, 2011; revised October 24, 2011, December 30, 2011, and February 11, 2012; accepted March 24, 2012. Date of publication July 6, 2012; date of current version December 19, 2012. This work was supported by the Natural Sciences and Engineering Research Council of Canada, Environment Canada, the Canadian Space Agency, Agriculture and Agri-Food Canada, the National Aeronautics and Space Administration, and the U.S. Department of Agriculture.

R. Magagi, K. Goïta, I. Gherboudj, N. Djamaï, and L.-P. B. Rousseau are with the Département de Géomatique Appliquée, Université de Sherbrooke, Sherbrooke, QC J1K 2R1, Canada (e-mail: Ramata.Magagi@usherbrooke.ca; kalifa.goita@usherbrooke.ca; Imen.Gherboudj@USherbrooke.ca; Najib.Djamai@USherbrooke.ca; Louis-philippe.b-rousseau@usherbrooke.ca).

A. A. Berg and J. Belanger are with the Department of Geography, University of Guelph, Guelph, ON N1G 2W1, Canada (e-mail: aberg@uoguelph.ca; jBelanger@uoguelph.ca).

S. Bélair is with the Meteorological Research Branch, Environment Canada, Dorval, QC H9P 1J3, Canada (e-mail: stephane.belair@ec.gc.ca).

T. J. Jackson, M. H. Cosh, and I. Mladenova are with Hydrology and Remote Sensing Laboratory, USDA-ARS, Beltsville, MD 20705 USA (e-mail: tom.jackson@ars.usda.gov; Michael.Cosh@ars.usda.gov; iliana.mladenova@ars.usda.gov).

B. Toth is with MSC Hydrometeorology and Arctic Lab, Environment Canada, Saskatoon, SK S7N 3H5, Canada (e-mail: brenda.toth@ec.gc.ca).

A. Walker is with Climate Research Division, Environment Canada, Toronto, ON M3H 5T4, Canada (e-mail: anne.walker@ec.gc.ca).

H. McNairn, J. Shang, and A. Merzouki are with Agriculture and Agri-Food Canada, Ottawa, ON K1A 0C6 Canada (e-mail: heather.mcnairn@agr.gc.ca).

P. E. O'Neill is with the Hydrological Sciences Branch, Laboratory for Hydrospheric Processes, NASA Goddard Space Flight Center, Greenbelt, MD 20771 USA (e-mail: peggy.e.oneill@nasa.gov).

M. Moghaddam and M. Burgin are with the Department of Electrical Engineering and Computer Science, University of Michigan, Ann Arbor, MI 48109-2122 USA (e-mail: mmoghadd@eecs.umich.edu; mburgin@umich.edu).

A. Colliander, J. B. Fisher, and S.-B. Kim are with the Jet Propulsion Laboratory, California Institute of Technology, Pasadena, CA 91109 USA (e-mail: andreas.colliander@jpl.nasa.gov; Joshua.B.Fisher@jpl.nasa.gov; seungbum.kim@jpl.nasa.gov).

Color versions of one or more of the figures in this paper are available online at http://ieeexplore.ieee.org.

Digital Object Identifier 10.1109/TGRS.2012.2198920

I. Introduction

Remote sensing of soil moisture is a key component of several observing and research programs including the Global Energy and Water Cycle Experiment (GEWEX), the Integrated Global Water Cycle Observation (IGWCO), and the Global Soil Wetness Project (GSWP), among others. This is related to the fact that soil moisture plays a critical role in governing global water and energy cycles. Recently, Jung *et al.* [1] linked the decline in global evapotranspiration since 1998 to a potential limitation in soil moisture supply. At regional and local scales, soil water availability affects the distribution of vegetation and crop health and impacts flood risk. Bélair *et al.* [2] and Koster *et al.* [3] have shown the importance of the initial soil moisture state for improved climate and weather forecasts, while Berg and Mulroy [4] have demonstrated the value of modeled soil moisture for improving streamflow forecasts. Numerous previous and current microwave satellite missions (RADARSAT-2, AMSR-E, ALOS-PalSAR, etc.) provide data which can be used to estimate and monitor changes in soil moisture. In addition, the European Space Agency's (ESA) new Soil Moisture and Ocean Salinity (SMOS) mission and the National Aeronautics and Space Administration's (NASA) proposed Soil Moisture Active and Passive (SMAP) mission are dedicated to monitoring global soil moisture information [5]–[7]. Exploitation of this new satellite microwave data requires intensive campaigns to collect ground and airborne data to validate SMOS brightness temperature data and soil moisture products. Lessons learned from SMOS investigations, particularly when complemented with airborne radar data, will contribute to SMAP algorithm development and validation.

Several international field experiments, over a variety of landscapes, have been devoted to the assessment of SMOS brightness temperature data and soil moisture products. Each of these has value for the overall assessment of the SMOS products. The Canadian Experiment for Soil Moisture in 2010 (CanEx-SM10) complements these by focusing on a different climate region. Details on these field campaigns can be found in [8]–[14].

The purpose of this paper is to present an overview of CanEx-SM10 [12], which took place from 31 May to 16 June 2010 in Saskatchewan, Canada. CanEx-SM10 was a collaborative effort between researchers in Canada and the United States. The campaign was designed to collect field measurements for both the validation of SMOS data and the prelaunch assessment of planned SMAP soil moisture products. Another objective was to contribute to the development of soil moisture retrieval algorithms specifically for agricultural and boreal forest areas in Saskatchewan, Canada. To meet these objectives, L-band passive microwave data were acquired with a radiometer mounted on a Twin Otter aircraft owned by the National Research Council of Canada (NRC) and managed by Environment Canada (EC). Data were also acquired by NASA's Uninhabited Aerial Vehicle Synthetic Aperture Radar (UAVSAR), which is a polarimetric L-Band SAR sensor flown on a Gulfstream-III (G-III) aircraft. Coincident with airborne and satellite (SMOS, AMSR-E, RADARSAT-2, and ALOS-PalSAR) acquisitions, ground measurements were made to characterize the soil (moisture, temperature, roughness, bulk density) and the vegetation (height, biomass, leaf area index (LAI), density). In addition, two ground-based networks managed by the University of Guelph (U of G) and EC provided continuous measurements of soil moisture over the study area. At the time of the present study, SMOS is in its early operational phase (since June 2010) and, consequently, the large data set collected during CanEx-SM10 provides critical data to improve the soil moisture retrieval algorithms for both agricultural and boreal forest landscapes and to develop downscaling approaches. The large agricultural fields (approximately 60 ha), characteristic of Canada's Prairies region, are well suited to address L-band coarse resolution passive microwave research questions. CanEx-SM10 was the first attempt in Canada to acquire soil moisture observations simultaneously with satellite and aircraft microwave measurements for the development of large-scale soil moisture retrieval algorithms. In addition, considering SMOS calibration and validation activities and the prelaunch assessment of the proposed SMAP mission, CanEx-SM10 is one of the few soil moisture experiments conducted over a boreal forest and subarctic environment.

The following sections describe the CanEx-SM10 study sites and the experimental design, including the sampling strategy associated with the ground and airborne measurements and the selection of SMOS and other satellite acquisitions. The analysis of data collected during CanEx-SM10 is then presented followed by a short description of the CanEx-SM10 database.

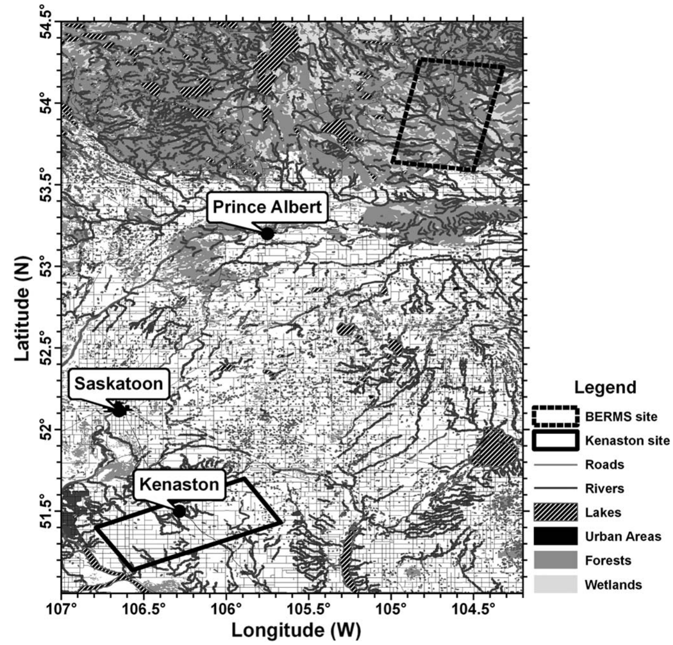

Fig. 1. CanEx-SM10 study area including both the Kenaston agricultural site and BERMS boreal forest site.

II. Sites

A. General Description of the Study Sites

The CanEx-SM10 experiment was conducted over two disparate landscapes including an agricultural and a forested region of Saskatchewan, Canada (Fig. 1). Both the agricultural Kenaston site and the forested site of the Boreal Ecosystem Research and Monitoring Sites (BERMS) covered an area of 33 km $\times$ 71 km (about two SMOS pixels). These sites were selected to minimize as much as possible large lakes, which can be problematic for the validation of coarse resolution microwave data.

In addition, the following aspects were considered during the selection of the two study sites:

- Both the Kenaston and BERMS sites benefit from long-term *in situ* soil moisture measurement networks, which are managed by EC at BERMS and by EC and the U of G at Kenaston. Meteorological stations are also available.
- The cropping system present within the Kenaston site is very typical of the Canadian Prairie region, consisting of cereal, oilseed, and pasture-forage crops. Fields in this region are considered large, reaching 60 ha in size. The cropping mix and field sizes of the Kenaston area are well suited for testing the retrieval algorithms of soil and vegetation parameters from microwave remote sensing.
- The BERMS site benefits from long-term ecological data collected during previous research programs such as the Boreal Ecosystem-Atmosphere Study (in 1994 and 1996) and BERMS (1996 to present).

1) Kenaston Site: The agricultural site (Fig. 1) is located approximately 80 km from Saskatoon (52.12 N, 106.63 W), Saskatchewan, Canada. The topography of the region (downloaded from [15]) is shown in Fig. 2(a). As evident in this figure, the region is not perfectly flat, and the highest elevations are in the eastern part of the area, and there is a valley toward

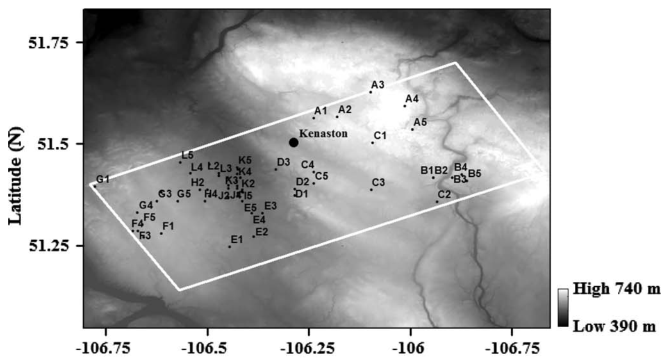

(a)

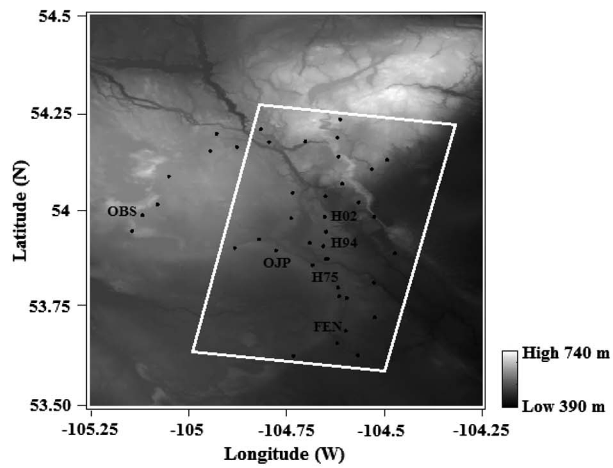

(b)

Fig. 2. (a) Digital elevation model of the Kenaston site at 30-m resolution (downloaded from [15]) along with the location of the sampling stations (♦). Basic information for all the stations is provided in Table I. (b) Digital elevation model of the BERMS site at 30-m resolution (downloaded from [15]) along with the location of the sampling stations (♦). OBS, HO2, H94, OJP, H75, and Fen are BERMS permanent stations. Basic information for all the stations is provided in Table II.

the west. Based on Landsat image classification, approximately 92% of the site is under annual cultivation with most of the remaining area in permanent grass and pasture. Production is almost exclusively rain-fed with minimal use of irrigation. Prior to and during the CanEx-SM10 experiment, the Kenaston area experienced above normal rainfall resulting in very wet soil conditions. As a consequence, pools of standing water were present in many fields, increasing the percentage of open water from 1.5% to 4.9% [16], [17]. The presence of standing water inevitably complicates the analysis and interpretation of the coarse resolution microwave signals.

Table I describes the field conditions during CanEx-SM10. With the exception of the pasture fields, most fields had been tilled and were covered with varying amounts of crop residue. Seeding and crop development were delayed in the spring of 2010 due to the unusually wet soil conditions. Vegetation cover varied but was less than 50% for most fields (Table I). Although most of the soils are loamy, high variability was observed in soil texture, and the dominant textures included silt, clay, and sandy loams.

2) BERMS Site: The BERMS region is located north of Prince Albert (53.24 N, 105.75 W) in Saskatchewan near the southern extent of the boreal forest (Fig. 1). BERMS features several instrumented research sites located in areas with various vegetation types (mostly forest), ages, and structures [18]. The topography (downloaded from [15]) is generally rolling [Fig. 2(b)], and the dominant vegetation type depends on the soil types and drainage conditions. To reduce the contribution of lakes to the observed microwave signals, CanEx-SM10 only covered the eastern portion of the study area which was originally defined for the BERMS measurements program [16]. Five vegetation types (old Aspen, old Jack Pine, Harvested Jack Pine, Fen, and old Black Spruce) mostly forests are dominant in this region (Table II).

B. Ground Truth Locations

Measurements to characterize the soils and vegetation were spatially distributed over the Kenaston and BERMS sites, capturing the natural variability in the landscape. Sampling stations were selected based upon availability of resources, road accessibility, and ability to meet two objectives: 1) provide a suitable data set to validate satellite and airborne soil moisture retrieval; and 2) relate point measurements to satellite acquisitions. For soil moisture and vegetation characteristic measurements (Table III), a total of 60 fields (Table I) were sampled over the Kenaston site. These included 24 fields instrumented with long-term *in situ* soil moisture stations managed by EC and 16 fields instrumented and managed by U of G. An additional 20 fields were added to complement these permanent sites. The spatial distribution of the sampling fields for the Kenaston area is shown in Fig. 2(a).

For the BERMS site, there were 35 sampling stations [Fig. 2(b)] consisting of six BERMS permanent stations (OBS, HO2, H94, OJP, H75, and Fen) located at BERMS research sites, 20 BERMS temporary stations installed by the U.S. Department of Agriculture (USDA) from May to August 2010 and several ground truth sites. All 35 stations were sampled on the airborne flight day [16] for soil moisture and temperature measurements (Table III). Vegetation characteristic measurements were only conducted for the BERMS permanent stations (Table II).

III. Experimental Design

CanEx-SM10 was an intensive short-term campaign (31 May to 16 June, 2010) designed to collect consistent field measurements at a time close to satellite and airborne acquisitions to support validation of both SMOS and planned SMAP products. Table III presents a comprehensive list of the field data collected during CanEx-SM10. The spatial extent of both the Kenaston and BERMS sites was equivalent to about two SMOS pixels. The size of the study sites impacted the experimental design and was a factor in optimizing the number of sampled stations. This optimization included minimizing sampling times and travel time from one field to another as well as coordinating sampling to be coincident with SMOS overpasses, all within available resources. Given these constraints and the requirement to collect spatially distributed soil and vegetation measurements (moisture, roughness, biomass, LAI, bulk density, etc.), the priority was to cover a large number of fields at the SMOS scale of approximately 30 km. A calendar of data collection and information on the available airborne and satellite acquisitions are provided in Table IV.

TABLE I
CHARACTERISTICS OF THE SAMPLING FIELDS OVER KENASTON AREA—24 EC FIELDS, 16 U OF G FIELDS, AND 20 MANUAL SURVEY (MS) FIELDS

				Crop				Soil					
Field type	**Field #**	**Lat (°N)**	**Long (°W)**	**Type**	**Height cm**	**Fractional cover %**	**Residue cover %**	**Bulk density g/cm³**	**Sand %**	**Silt %**	**Clay %**	**Type**	**Tillage**
EC	D4	51.25	106.45	Canola	-		>50	1.18	26	51	23	Silt Loam	Yes
	H1	51.39	106.52	Canola	-	5-11	<25	1.18	42	41	17	Loam	No
	H2	51.37	106.50	Canola	-	8	>50	1.12	39	44	17	Loam	No
	H3	51.36	106.51	Canola	-	12-35	>50	1.17	34	50	16	Loam	No
	H4	51.37	106.45	Cereal	2		25-50	1.14	50	32	18	Loam	Yes
	H5	51.38	106.43	Canola	1	15	25-50	1.19	37	41	22	Loam	No
	I1	51.37	106.43	Wheat	-	-	<10	0.87	28	59	13	Silt Loam	No
	I2	51.38	106.42	Wheat	8-10	1	<25	1.20	45	22	33	Clay Loam	No
	I3	51.39	106.41	-	-	-	<10	0.98	28	53	19	Silt Loam	No
	I4	51.38	106.41	-	-	-	<10	0.92	29	53	18	Silt Loam	No
	J1	51.39	106.45	Wheat	-	9	>50	1.19	23	57	20	Silt Loam	No
	J2	51.40	106.43	Wheat	-	18	>50	1.31	26	50	24	Loam	Yes
	J3	51.39	106.43	Canola	-	7-15	>50	1.34	31	46	23	Loam	No
	J4	51.41	106.43	Canola	4	11	>50	1.32	37	40	23	Loam	No
	J5	51.42	106.42	Wheat	-	3-7	>50	1.30	33	46	21	Loam	No
	K1	51.42	106.42	Wheat	3	-	>50	1.14	29	49	22	Loam	Yes
	K2	51.43	106.43	Peas	-	2.25	>50	1.09	20	43	37	Clay Loam	No
	K3	51.44	106.43	Canola	1	9-17	>50	1.06	33	47	20	Loam	No
	K4	51.44	106.43	Peas	3	7	>50	1	21	53	26	Silt Loam	No
	K5	51.45	106.50	Canola	3	6	>50	1.16	-	-	-	-	Yes
	L1	51.43	106.47	Wheat	25-30	60-80	<25	1.11	26	55	19	Silt Loam	No
	L2	51.42	106.47	Wheat	10-15	40	<25	1.13	29	49	22	Loam	Yes
	L3	51.43	106.54	Wheat	6-8	10-13	<25	1.09	34	45	21	Loam	No
	L4	51.45	106.57	Canola	4-5	15	>50	1.03	37	42	21	Loam	Yes
U of G	A2	51.57	106.18	Wheat	8-10	9-38	>50	1.26	29	42	29	Clay Loam	No
	A3	51.63	106.10	Pasture	10-25	38	25-50	1.13	-	-	-	-	No
	A4	51.59	106.01	No crop	-	-		-	-	-	-	-	
	A5	51.54	105.99	Peas	2	5-10	25-50	1.10	45	31	24	Loam	No
	C1	51.36	105.94	Pasture	20-25	50-73	>10	1.25	41	38	21	Loam	No
	C2	51.39	106.10	Not planted	-	-	>50	1.08	41	38	21	Loam	No
	C3	51.43	106.24	Wheat	8-10	8-14	<25	1.24	32	40	28	Clay Loam	No
	C5	51.37	106.29	Wheat	-	8-10	>50	1.03	20	53	27	Clay Loam	Yes
	E1	51.27	106.39	Pasture	-	-	<25	1.24	25	54	21	Silt Loam	No
	E4	51.36	106.41	Bare soil	-	-	>50	1.23	23	59	18	Silt Loam	No
	F2	51.28	106.67	Canola	-	9-15	25-50	1.10	30	49	21	Loam	Yes
	G2	51.36	106.63	Lentil	2-3	11	>50	1.21	34	48	18	Loam	Yes
	G4	51.36	106.57	Peas	3-4	15	>50	1.14	31	52	17	Silt Loam	No
	G5	51.39	106.50	wheat	-	13	>50	1.15	28	47	25	Loam	No
	L5	51.56	106.24	Lentil	-	7	>50	1.31	38	43	19	Loam	No
	I5	51.40	106.45	-	-	-	<10	1.02	30	54	16	Silt Loam	No
MS	A1	51.56	106.24	No crop	-	-	>50	1.12	40	39	21	Loam	Yes
	A6	51.42	105.94	No crop	-	-	25-50	1.12	35	38	27	Clay Loam	No
	B1	51.42	105.94	Pasture	-	39	<10	1.33	58	28	14	Sandy Loam	No
	B2	51.42	105.90	Pasture	-	54	<10	1.34	72	17	11	Sandy Loam	No
	B3	51.42	105.87	Pasture	10-40	23-75	<10	1.12	50	39	11	Loam	No
	B4	51.41	105.86	Pasture	-	28-50	<10	1.21	56	30	14	Sandy Loam	No
	B5	51.50	106.09	Pasture	-	7-22	>50	1.04	-	-	-	-	No
	C4	51.40	106.24	Bare soil	-	-	>50	1.23	33	41	26	Loam	Yes
	D1	51.39	106.29	Lentil	2-3	4	>50	1.16	30	43	27	Clay Loam	Yes
	D2	51.44	106.33	Canola	-	6	25-50	1.10	37	42	21	Loam	Yes
	D3	51.42	106.45	wheat	4	11	25-50	1.18	34	39	27	Clay Loam	Yes
	E2	51.33	106.36	Bare soil	-	-	>50	1.32	31	51	18	Silt Loam	No
	E3	51.33	106.39	Lentil	-	-	>50	1.19	23	54	23	Silt Loam	No
	E5	51.28	106.61	Wheat	4-8	7	25-50	1.26	28	51	21	Silt Loam	Yes
	F1	51.27	106.66	lentil	3	9	>50	1.21	42	40	18	Loam	No
	F3	51.29	106.68	Not planted	-	8	>50	1.27	37	45	18	Loam	No
	F4	51.30	106.66	Not planted	-	-	>50	1.23	39	47	14	Loam	No
	F5	51.39	106.78	Lentil	3	20	25-50	1.17	38	46	16	Loam	Yes
	G1	51.38	106.61	Not planted	-	-	>50	1.25	33	49	18	Loam	No
	G3	51.33	106.67	Not planted	-	-	>50	1.13	32	46	22	Loam	No

A. Ground Data Sampling Strategy

1) Soil Moisture, Temperature, and Bulk Density: For the Kenaston area, soil moisture, bulk density, and temperature were measured approximately coincident with the satellite and airborne acquisitions on 2, 5, 6, 7, 9, 13, and 14 June, 2010 (Table IV). On each sampling day, measurements were taken on 48–60 fields, with each team of two visiting four to five fields. The location of each sampling point in each field was recorded using a GPS. During subsequent sampling days, these coordinates were used to navigate to the same point, ensuring that each successive measurement was taken at the same location.

TABLE II
DESCRIPTION OF THE FIVE BERMS SAMPLING SITES AND THE MEASURED SPECIFIC PROPERTIES

Site_ID	Site description	Geographic location	Mean height	Mean DBH	Trunk density	Tree cover	Necromass cover	Understory cover	Litter depth
OBS	Mature wet old black spruce with moss and Labrador tea understory	53.99 N 105.12 W	7.1 m	7.33 cm	0.655 #/m^2	94.7 %	3.7 %	28.2%	18.54cm
OJP	Old dry jack pine with lichen understory	53.92 N 104.69	13.4 m	13.64 cm	0.225 #/m^2	88.7 %	6.0%	33.0%	7.11 cm
HO2	Harvested jack pine 2002 with ground cover consisting of sparse grass, shrubs and immature jack pine seedlings	53.95 N 104.65 W	1.82 m	2.38 cm	0.36 #/m^2	38.4%	19.6%	1.9%	0.6 cm
Temp7	Mixed Forest consisting of pine, fir and aspen	53.90 N 104.88 W	6.44 m, 6.87 m and 10.17 m respectively for pine, fir and aspen	7 cm, 7.9 cm and 9.2 cm respectively for pine, fir and aspen	0.43 #/m^2, 0.16 #/m^2 and 0.33 #/m^2 respectively for pine, fir and aspen	24.17 %, 75.92 % and 59.52 % respectively for pine, fir and aspen	7.03 %, 16.30 % and 15.17 % respectively for pine, fir and aspen	84.03 %, 34.66 % and 47 % respectively for pine, fir and aspen	17 cm, 4.58 cm and 3.36 cm respectively for pine, fir and aspen
FEN	Flooded vegetation, among others horse tail and grass and 2-3 kind of shrubs.	53.78 N 104.62 W	35.6 cm, 45.7 cm and 43.2-96.5 cm respectively for horse tail, grass and shrubs	0.285 cm, 0.08 cm and 0.37 cm respectively for horse tail, grass and shrubs	0.9 #/m^2, 3 #/m^2 and 0.1 #/m^2 respectively for horse tail, grass and shrubs	N/A	N/A	N/A	N/A

TABLE III
GROUND DATA COLLECTED AT THE KENASTON AND BERMS SITES

Sites	**Measurements**	**Human resource**	**Sampled stations**
Kenaston 1-14 June 2010	Soil moisture at 6-cm depth, bulk density, soil temperature at 5 and 10-cm depth, and Thermal Infra Red (TIR)	12 teams of 2 people	48-60 per sampling day
	Soil texture	12 teams of 2 people	60 for the entire campaign
	Vegetation (water content, height, density, etc.) and soil roughness	2 teams of 2 people	60 for the entire campaign
	Leaf Area Index (LAI)	3 people	60 for the entire campaign
BERMS 16 June, 2010	Soil moisture, soil temperature at 5 and 10-cm depth, surface temperature and TIR	6 teams of 2 people	35-40 for the sampling day
14-16 June and on 13-20 July, 2010	Tree characteristics (DBH, height, crown fractional cover, stem density, and branch measurements) and Soil moisture at 5 cm depth	1 team of 5 people	5
14-16 June and on 13-20 July, 2010	Understory characteristics (type, fractional cover), necromass cover, litter depth	1 team of 5 people	5

TABLE IV
AVAILABLE GROUND, AIRBORNE, AND SATELLITE MEASUREMENTS DURING CanEx-SM10

Measurements	**Sites**	**Kenaston**														**BERMS**
	June 2010	**1**	**2**	**3**	**4**	**5**	**6**	**7**	**8**	**9**	**10**	**11**	**12**	**13**	**14**	**16**
Ground Data Collection		-	√	-	-	√	√	√*	-	√	-	-	-	√	√	√
Satellite	SMOS	√√	√	√√	-	√√	-	√	√√	-	√√	√	√	√√	-	√√
	AMSR-E	√√	√√	√√	√	√√	√√	√√	√√	√√	√√	√√	√√	√√	√√	√√
	RADARSAT-2	√√	√	-	-	√√	-	-	√√	-	-	√	√	-	-	-
	ASAR	-	-	-	-	-	√	√	-	-	√√	-	-	√	-	√
	ALOS-PALSAR	-	-	-	-	-	√	√	-	√	-	-	-	-	√	-
Airborne	Twin Otter and UAVSAR	-	√	-	-	√	√	√*	-	√	-	-	-	√	√	√

√: one acquisition per day
√√: two acquisitions (ascending and descending) per day
√*: Partial coverage due to rain event

TABLE V
SAMPLING REGIMES OVER THE KENASTON AND BERMS STUDY SITES

Sites	Soil sampling regime	
Kenaston	Sampling points per field:	14 located at pre-programmed GPS points
	Transects per field:	2 transects 400 m apart
	Points per transect:	7
	Spacing between points in transect:	100 m with the first point 50 m from the field edge
	Number of soil moisture readings per point	3 (top, bottom and side of furrow)
	Soil moisture measurements	Probe inserted vertically, soil moisture is integrated over 6 cm
	Soil temperature	4 points at two depths (5 cm and 10 cm)
	Thermal infra red (TIR)	4 measurements in each field. Exposed Vegetation, shaded vegetation, exposed ground, and shaded ground.
	Bulk Density	1 core sample of 5 cm depth
	Site Photos	One taken in the direction of the crop row,
BERMS	Sampling points per GTS:	3, located at pre-programmed GPS points
	Spacing between points:	5 m (20 m, 25 m and 30 m from the GTS)
	Number of soil moisture readings per point	3 (top, left and right side of measurement point)
	Soil moisture measurements	Probe inserted vertically, soil moisture is integrated over 6 cm
	Soil temperature	Simultaneously to soil moisture at 5 cm depth
	Thermal infra red (TIR)	4 Measurements for each GTS. exposed vegetation, shaded vegetation, exposed Ground, and shaded ground.
	Gravimetric soil moisture	3 samples of 5 cm depth per GTS
	Site Photos	Two landscape and one vertical
Kenaston	**Vegetation sampling regime**	
	Vegetation characterization	plant density, row spacing, row direction
	Wet and dry biomass and canopy water content	1 m sampling if rows were well defined, otherwise sample of 50 cm x 50 cm using a gridded board, 3 replicates. Wet samples oven dried to determine dry biomass and canopy water content.
	LAI	14 hemispherical photos along 2 parallel transects 30 m in length
	Site photos	1 photograph of a gridded board placed over the vegetation, 3 replicates; 14 crop architecture photos
	Vegetation height and stem diameter	3 – 10 height and diameter measurements per site at each of three sites
BERMS	Transects per site:	3 of 100 m length for the mixed forest (Temp 7) and 1 of 100 m length for OBS, OJP, and HO2 sites
	Spacing between points in transect:	10 m
	Vegetation characterization	Species identification, tree height, % cover, diameter-at-breast-height (DBH), tree count, crown depth, litter depth, necromass and understory covers
	Densities of stems, large and small branches, leaves	From tree trunk density
	Radius and length of large and small branches, leaves	From a destructive sampling of one 'average' tree
	Distribution parameters	From photographs and site inspection

In each field, soil moisture was measured to a depth of 6 cm using the Steven's Water Hydra Probe inserted vertically. Sampling was conducted along two transects 400 m apart. Each transect included seven sample points at a 100-m spacing. At each sample point, three replicate moisture readings were collected. When tillage structure was evident, these replicates were located at the top, bottom, and side of the tillage furrow. Table V presents the sampling regime for soil moisture, soil temperature, thermal infra red (TIR), and bulk density at Kenaston. For each field and on each sampling day, a gravimetric sample was obtained for a fixed volume of the surface layer. These samples were taken to the laboratory for oven drying over a 24-h period. Then, they were used to calibrate the soil moisture probes and to derive soil texture and bulk density via lab analysis.

In addition to the manual sampling of soil moisture within each field, hourly soil moisture and soil temperature profiles at 5, 25, and 50-cm depths were recorded continuously at single points by the EC and U of G networks. They also used the Steven's Water Hydra probes installed vertically and horizontally for, respectively, EC and U of G networks. Using the calibration curves developed for each network station, uncertainty in volumetric soil moisture ranged from $\pm 0.03\ \mathrm{m^3/m^3}$ to ± 0.015–$0.02\ \mathrm{m^3/m^3}$, depending on the soil texture [19]. Some additional details regarding the network operated by the U of G are described in [20]. These profiles of soil moisture and soil temperature were complemented by precipitation measurements from rain gauges.

Over BERMS, a one-day field campaign was conducted on 16 June 2010. Soil moisture, bulk density, and temperature measurements were collected approximately coincident with the aircraft and SMOS acquisitions. In the sampling approach for this site, measurements were taken at 35 ground truth stations (GTS) that were spatially distributed over the study area and located along accessible roads and trails [16]. At each GTS station, three soil moisture measurements were taken at a 6-cm depth and at three measurement points located within the surrounding canopy at a nominal distance of 20, 25, and 30 m from the GTS location. The sampling was conducted by six teams of two people and covered the entire area, within the limits of road inaccessibility. Table V presents the sampling strategy for soil moisture, soil temperature, TIR, and bulk density at BERMS. As at the Kenaston site, preprogrammed GPS coordinates were used to easily and accurately geolocate the sampling stations. In some cases, the collection of bulk density samples over BERMS was complicated by the presence of an organic layer of variable thickness. At each of the three replicate sampling locations, the organic layer was first measured and then removed from a 20 cm $\times$ 28 cm area in order to collect a sample of the underlying mineral soil from which the bulk density was derived. The depth of the organic layer was recorded and the material bagged and weighed for the determination of water volume.

The above data sets were augmented with soil moisture and soil temperature which are continuously collected at different depths and at 4-h intervals at the permanent BERMS research stations [18]. The only exception was the Fen site where data were recorded every 30 min. Furthermore, over BERMS, CanEx-SM10 also benefited from 5-cm depth soil moisture measurements collected on an hourly time interval at 20 temporary stations [16].

2) Soil Roughness: The soil roughness measurements were made over the Kenaston fields using a 1-m pin profiler consisting of 200 needles spaced at an interval of 5 mm. Each field was sampled at least once, however, resampling was conducted over fields that were tilled during the campaign. The objective was to measure soil roughness characteristics (standard deviation (STD) of surface heights and correlation lengths) to quantify the impact of roughness on SAR backscatter and to a lesser extent on L-band passive microwave data for estimating soil moisture at the SMOS scale. Due to the expanse of the study area (about two SMOS pixels), an approach was adopted to optimize the number of roughness measurements across the site. Data collected in July of 2008 over Kenaston was analyzed to determine the within field variance in surface roughness to guide the sampling design. This analysis determined that the within field variance in roughness is far less than the field to field variance. Roughness in agricultural regions is largely driven by tillage applications, and thus this observation is not unexpected. Based on this analysis, it was determined that one sample site per field was sufficient to characterize roughness. The pin profiler is positioned perpendicular to the soil, and once the board is level, the needles are released. The tops of the needles mimic the surface roughness profile. At each site, a 3-m roughness profile was created by placing the 1-m profiler end to end in the look directions of both the UAVSAR and RADARSAT-2 (descending overpass). This 3-m profile was replicated three times, at a distance of approximately 5 m. A digital camera recorded the pin meter profiles, and these photos were processed to derive surface roughness characteristics (STD of surface heights and correlation lengths). Processing of the photos and the extraction of the roughness statistics are described in [21]. The mean and the STD of the surface roughness parameters were computed to determine the average field roughness.

Over the BERMS forested site, no roughness measurement was collected due to the presence of an understory.

3) Vegetation: The Kenaston data will be used to assess the impact of canopy water content on the microwave response in estimating soil moisture at SMOS and planned SMAP scales. For each field, three replicate vegetation samples were gathered at a single site. Measurements of plant height, stem diameter, plant density, row spacing, and row direction were recorded. To minimize crop disturbance, vegetation in front of the 1-m pin profiler was removed, providing a measurement of above ground wet biomass. The vegetation samples were oven-dried at 80 °C to constant weight, which provided both dry biomass weights and canopy water content. Due to time constraints, each field was sampled once for the derivation of the aforementioned parameters.

In addition to destructive vegetation sampling, crop development was also monitored with the measurements of LAI. At each site, a total of 14 hemispherical photos were taken at 5 meters spacing along two parallel transects approximately 35 m long and 5 m apart. This method of LAI determination was well-suited conditions in this experiment given the limited canopy development. Coincident with the LAI measurements and accompanying each set of hemispherical photos, crop architecture photos were also collected at each site. A summary of the sampling of vegetation characteristics is given in Table V.

BERMS data will be used to investigate how well soil moisture can be retrieved in boreal landscapes using L-band active/passive microwave remote sensing. The data will also assist in improving SMOS soil moisture retrieval algorithms, in developing the proposed SMAP soil moisture retrieval algorithms and in forward modeling of SMAP radar backscatter. At BERMS, a total of five sites were sampled (Table II). The ground measurements included three 100-m transects at a mixed forest site (Temp7) and one 100-m transect at each of the Old Jack Pine, Old Black Spruce, and Harvested Jack Pine sites. The Fen site vegetation characteristics were measured along the boardwalk leading to the flux tower location. Various vegetation measurements were taken in 10-m intervals along each transect (Table V). At every 10-m mark, tree height, trunk radius, and tree count were measured together with trees fractional cover, understory cover, necromass cover, and litter depth. The stem density along the entire transect was determined by counting the number of stems within a $\sim$2-m arm-span and dividing by the area (approximately 100 m $\times$ 2 m). The densities of large and small branches as well as that of leaves were calculated from the trunk density and the quantity of these components for the measured trees at each 10-m mark. Crown layer depth and trunk height, as well as trunk diameter-at-breast-height (DBH) were recorded. For each forested site, one "average" tree was destructively sampled from which the radius and length of large and small branches as well as leaf dimensions were recorded. The distribution parameters of the branches were deduced from photographs and inspection in the field.

B. Remote Sensing Data

To meet the objectives of CanEx-SM10, both airborne and satellite remote sensing data were acquired.

1) Aircraft Data: Two aircraft, one equipped with a passive microwave radiometer and the other with an active SAR, were used in CanEx-SM10. These included a Twin Otter aircraft owned by the NRC and managed by EC, and NASA's G-III aircraft. These aircrafts were deployed to acquire data to support the validation of SMOS products (L1, L2), the prelaunch assessment of planned SMAP data, and the evaluation of soil moisture retrieval algorithms from these two missions. The data will also be used to investigate approaches to scaling among remote sensing sources and to understand the relationship between ground measurements and satellite products. The Twin Otter and G-III attempted to cover the Kenaston and BERMS study areas close in time to SMOS overpasses. The flight calendar is presented in Table IV.

- Twin Otter: This aircraft was equipped with EC's passive microwave radiometers which operate at 1.4, 6.9, and 19–37–89 GHz. Visible and infra red radiometers were also mounted on the aircraft, and these sensors provide variable spectral information suitable to assist with data analysis and modeling. About 16 parallel flight lines were required to cover each study area. The L-band radiometer was flown at an altitude of approximately 2.3 km which resulted in a spatial resolution of about 2.25 km. These L-band data were collected at a 40° incidence angle.
- NASA G-III: This aircraft carried the UAVSAR which is a fully polarimetric L-band radar [22]. Using multiple flight lines, the UAVSAR provided spatial coverages similar to those of the L-band radiometer with a nominal flight altitude of 13 km. The UAVSAR collected data over a swath of about 21 km with the incidence angle ranging from 20° (near range) to 65° (far range). The pixel size is 7.5 m in range × 6 m in azimuth. The UAVSAR data are publicly available from the UAVSAR data server of the Jet Propulsion Laboratory (JPL) [22] for both the Kenaston and BERMS sites.

Full details on the flight lines of both the Twin Otter and the G-III as well as additional information on passive and active microwave sensors aboard these aircrafts can be found in the Experimental plan of CanEx-SM10 [16].

2) Satellite Data: SMOS acquisitions available over the study sites during CanEx-SM10 are listed in Table IV. Other satellite acquisitions (AMSR-E, RADARSAT-2, Envisat ASAR, and ALOS-PalSAR) were planned to be as close in time as possible to the SMOS overpasses. Several modes of RADARSAT-2 were planned including acquisitions of Fine Quad Polarimetric, Standard and Wide Swath, at varying incidence angles. Envisat ASAR acquisitions in Alternating Polarization and Wide modes were programmed to fill gaps in the RADARSAT-2 acquisition plan. ALOS-PalSAR data were acquired in Fine Dual and Wide modes. To maximize temporal coverage, whenever possible, both ascending and descending microwave acquisitions were programmed. L- and C-band microwave satellite data (Table IV) will be compared with L- and C-bands airborne data to understand the scaling effect on soil moisture and to develop active/passive soil moisture retrieval algorithms.

In addition to microwave satellite data, LANDSAT, SPOT, and AWiFS optical measurements were available over the Kenaston site.

IV. Preliminary Results

A. Ground Measurements

1) Soil Moisture, Bulk Density, and Temperature: Over the Kenaston fields, a site-specific calibration of the volumetric soil moisture measured by the Steven's Water Hydra Probes was performed using the gravimetric soil samples. Fig. 3 shows a summary of these data set and suggests a strong agreement between soil moisture measured by the two methods. The data spread observed around the 1:1 line can be attributed to variances in soil type and errors in collecting gravimetric samples and thus in estimating soil bulk density. The soil bulk density values derived from the gravimetric samples are presented in Table I for each field.

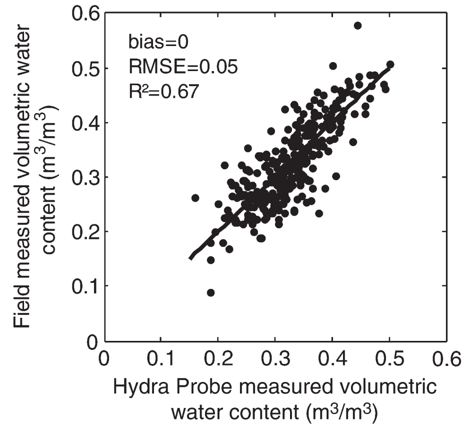

Fig. 3. Calibration curve of the hydra probe sensors over the Kenaston fields.

The individual field average soil moisture measured at Kenaston during CanEx-SM10 are presented in Fig. 4(a). The high soil moisture values reflect the very wet conditions due to heavy rainfall before and during the field campaign (Section II). Some variation in soil moisture is observed between fields. A number of factors contribute to interfield differences in wetness including topography, precipitation amounts, soil texture, and vegetation cover (Fig. 2 and Table I) and will be explored in greater detail in the future. As a complement of Fig. 4(a), the temporal evolution of the averages soil moisture, soil temperature, and precipitation data is given in Fig. 5. The lowest soil moisture conditions were observed for Julian Days 153 (2 June), 156 (5 June), and 157 (6 June). Rain on Julian Days 158 (7 June) and 159 (8 June) resulted in very wet conditions on Julian Day 160 (9 June). Warm and dry conditions observed after Julian Day 163 (12 June) led to the soil drying toward the conclusion of the experiment. Indeed, soil moisture values on Julian Days 164 (13 June) and 165 (14 June) were lower than the values observed on Julian Day 160 (9 June). Fig. 6 shows the coefficient of variation as a function of the mean soil moisture values for each field measured at Kenaston during CanEx-SM10; for each sampling day, each data point is the average of 14 soil moisture measurements for a given field (Section III-A1). These statistics indicate a decrease in the relative variation in soil moisture with an increase in moisture. Famiglietti *et al.* [23] have shown that this decrease in variance is reduced at higher moisture levels, within a range of 0.20–0.45 m^3/m^3 soil moisture. This suggests that other site factors may play a role and thus might explain the scatter observed in Fig. 6. The field to field variation of some of these factors is given in Table I. Current studies are focused on attributing the observed variance to physical processes.

Soil temperature was measured at a 5-cm depth simultaneous with the soil moisture measurements. The temporal trend in

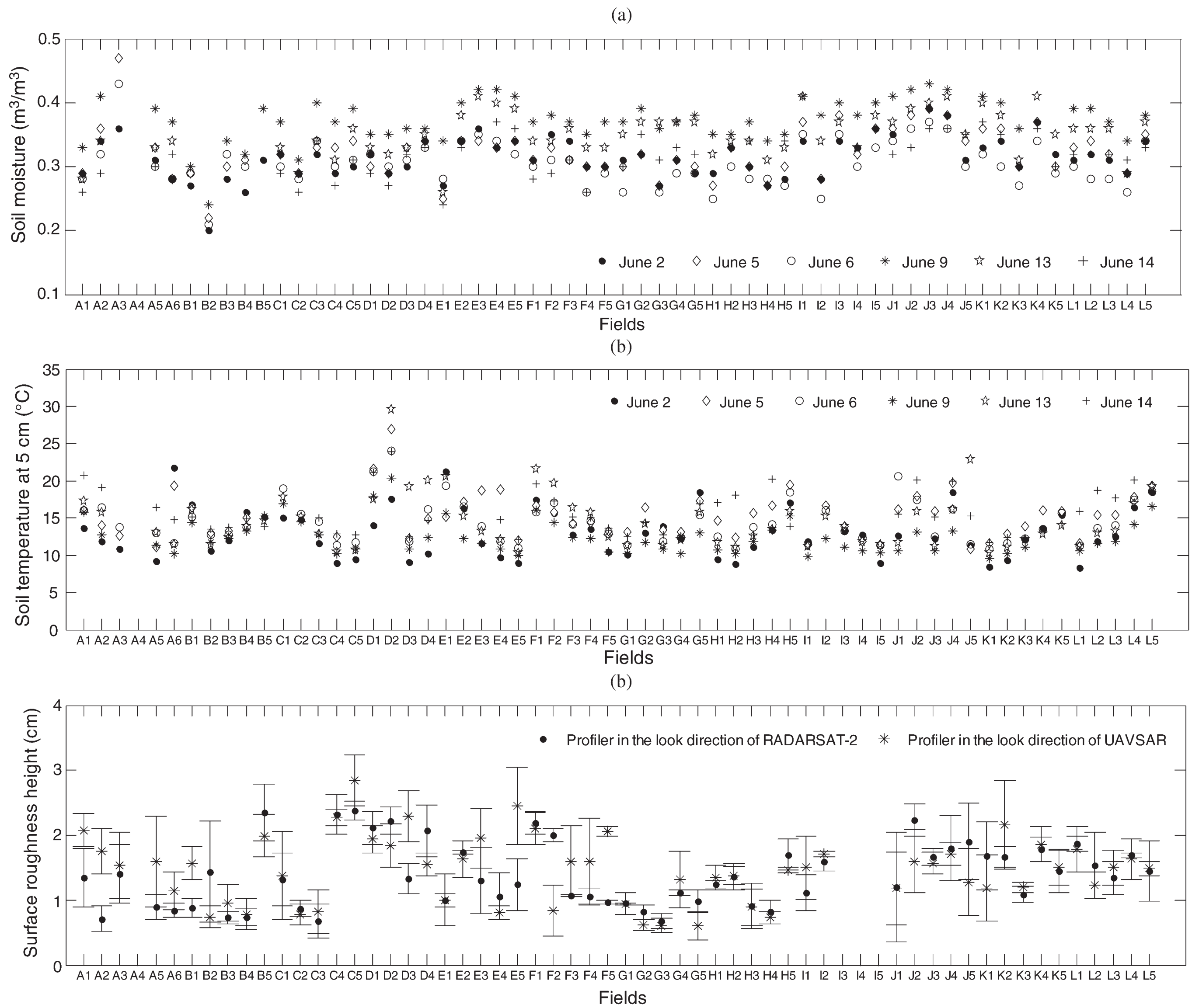

Fig. 4. Field average soil characteristics over Kenaston during CanEx-SM10. (a) 6-cm soil moisture, (b) 5-cm depth soil temperature, and (c) surface root mean square (rms) roughness height.

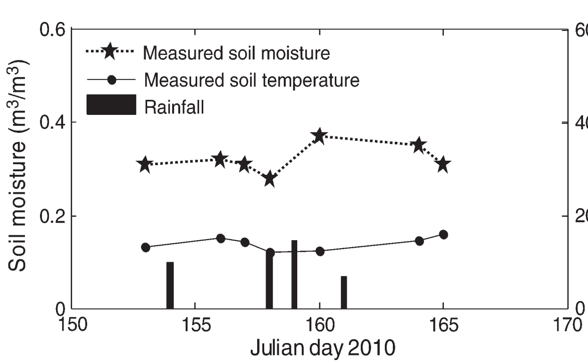

Fig. 5. Temporal evolution of the mean values of the measured soil moisture, soil temperature and precipitation over Kenaston during CanEx-SM10.

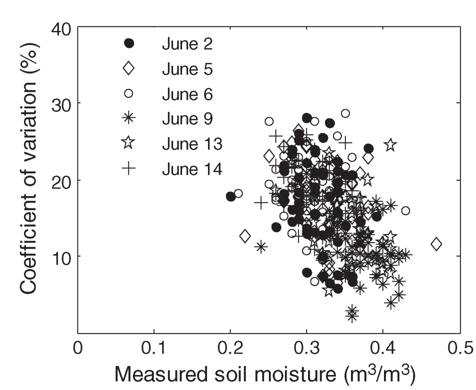

Fig. 6. Coefficient of variation in soil moisture *versus* the mean values of the measured soil moisture (m^3/m^3) during CanEx-SM10.

soil temperature matches that of soil moisture as presented in Fig. 4(a). The soil temperature ranged from 7 °C to 30 °C Fig. 4(b).

2) Soil Roughness: The measurements of soil roughness in the look direction of both RADARSAT-2 (91° in descending) and UAVSAR (242°) are shown in Fig. 4(c). In some cases, there was no significant macro tillage structure, and the two measurements were similar. In the fields with tillage structure, roughness did vary as a function of the SAR look direction.

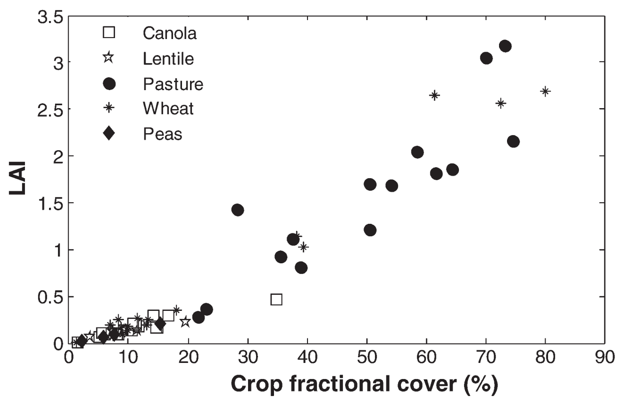

Fig. 7. Measured effective LAI versus percent crop fractional cover.

In addition, roughness measured in the look direction of the UAVSAR was higher than that measured in the look direction of RADARSAT-2. Consequently, a constant surface roughness cannot be assumed in backscatter modeling in this region.

3) Vegetation: Several vegetation characteristics were measured over the Kenaston and BERMS sites (Section III-A3). In this paper, the consistency of the data was evaluated empirically. For the Kenaston fields, Fig. 7 demonstrates a positive relationship between LAI and percent crop fractional cover. This is expected during early crop development, which was the CanEx-SM10 condition. At higher LAI, this relationship weakens as crop cover becomes near complete yet LAI continues to increase. However, the vegetation water content measurements were collected over few fields (∼12) for which the vegetation fractional cover exceeded 25%. The measurements varied from 0.04 to 1.69 kg/m^2 with a mean value of 0.42 kg/m^2. This information is not included in Table I due to the lack of data for most fields. Additional information on crop characteristics associated with the Kenaston fields are given in Table I.

Measurements and vegetation-specific properties collected over BERMS are described in Tables II and III. The biomass and the age of the forest sites were not recorded during CanEx-SM10. They can be retrieved from the FLUXNET database [24]. Tree heights varied from 1 to 22 m; tree heights were greatest at the OJP site (8–19 m) followed by the OBS site (2–13 m). Younger trees dominated the HO2 with tree heights varying from 1 to 3 m. In Table VI, the strong relationship between tree heights (in meters) and the DBH (in meters) is demonstrated for sites Temp 7, HO2, and OBS. A much weaker relationship is observed for the OJP site (Table VI). These relationships, known as allometric equations for trees, are very helpful in the remote sensing of forests since they allow us to overcome gaps in ground truth data and to estimate several tree characteristics due to their interdependence [25]–[28].

TABLE VI
RELATIONSHIPS DBH (D IN m) VERSUS TREE HEIGHT (H IN m) MEASUREMENTS AT DIFFERENT SITES OF BERMS

Sites	Tree species	Linear relationships
Temp 7	Pine (only)	D = 0.012H-0.009 ; R^2 = 0.81
OBS	Old Black Spruce	D = 0.011H-0.002 ; R^2 = 0.80
HO2	Harvested Jack Pine	D = 0.02H-0.012 ; R^2 = 0.84
OJP	Old Jack Pine	D = 0.0074H+0.038 ; R^2 = 0.41
OJP+ HO2	Old and harvested Jack Pine	D = 0.0096H+0.0069 ; R^2 = 0.94
All	All	D = 0.0096H+0.0065 ; R^2 = 0.82

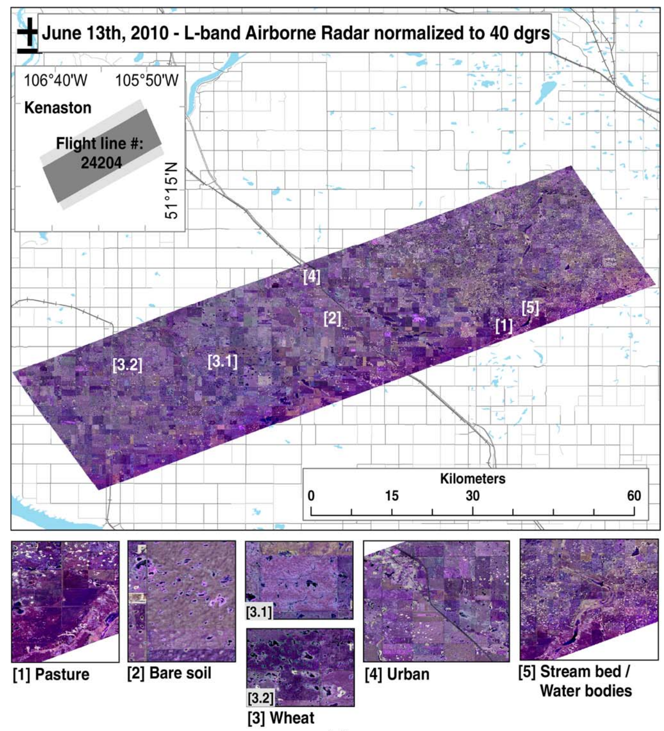

(a)

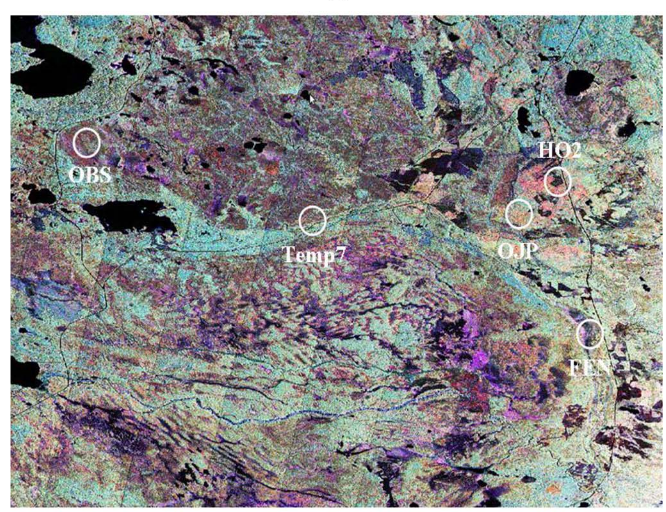

(b)

Fig. 8. (a) R-G-B color composite of UAVSAR 13 June, 2010 acquisition normalized at 40° over the Kenaston site. Additional information on the subplot locations obtained from Table I: [1] Sampling fields B1 and B2 (pasture); [2] Sampling field C4 (bare soils); [3] Sampling fields L2 (wheat-covered field, [3.1]) and G5 (saturated wheat-covered field with standing water present, [3.2]); [4] Kenaston city + major road infrastructure; [5] River bed + lake Vanzance. (b) Mosaic of UAVSAR 16 June, 2010 acquisition over BERMS site from individual data swaths with 25°–65° incidence angle range. R-HH, G-HV, and B-VV.

B. Remote Sensing Data

1) UAVSAR: The UAVSAR acquired data over the Kenaston site at incidence angles of 20°–65°. The original images were processed to produce a normalized data set with an incidence angle of 40° [29]. Fig. 8(a) is an R-G-B (HH-HV-VV) color composite of 13 June, 2010 acquisition. The extent of the UAVSAR coverage and its location within the Kenaston site are provided (upper left corner of the image) in Fig. 8(a). In this figure, the strongest response is observed for the HH (red color) and VV (blue color) polarizations, with much lower contributions from the HV (green color) channel. This indicates a dominance of surface scattering from bare or sparsely vegetated surfaces, with little contribution from volume scattering. Variations in the HH and VV responses are evident, and these reflect the field-to-field differences in soil moisture and roughness [Fig. 4(a) and (c)]. Very dark locations are often associated with specular reflection from standing water. In addition to capturing the ground conditions (i.e., soil moisture, vegetation cover) during the campaign, the UAVSAR data provide a basis for discriminating between the different ground cover types and terrain features encountered in the Kenaston domain. The radar response clearly shows differences between vegetated (Fig. 8(a), Locations [1] pasture fields and [3] wheat fields) and bare (Fig. 8(a), Location [2]) soils, and also reflects different moisture conditions (Fig. 8(a), Location [3], where the two subplots show the UAVSAR response measured over intermittently wet [3.1] and saturated [3.2] wheat field, respectively). In addition, the river bed which is clearly distinguishable in the DEM image [Fig. 2(a)] can also be easily identified in the UAVSAR map.

The UAVSAR data acquired over the BERMS site on 16 June 2010 can be seen in Fig. 8(b) where the individual data swaths with 25°–65° incidence angle range were postprocessed by georeferencing and assembling them into a single image mosaic to cover the whole area of interest. The image is an R-G-B (HH-HV-VV) color composite of 16 June 2010 acquisition. The location of the five BERMS sites sampled for vegetation can be identified by their location with respect to White Gull Lake, which shows up prominently in the image as a dark surface in the middle left of the image. The UAVSAR data show strong variations between the different vegetation types based on the combination of polarizations in the response and provide rich information content for use in quantitative retrieval and interpretation. Generally speaking, the darkest areas in the image correspond to bodies of water; bare soil surfaces and surfaces with grass or very short vegetation also appear dark, but not as much as the water surfaces. Since the VV response is generally stronger than HH and certainly HV, the bare surfaces though dark may appear with blue tones in the image. Forested areas with tall stems produce large amounts of the so-called "double-bounce" scattering, which is most pronounced in the HH channel and therefore contains a strong red component in the image. Locations with dense crown layers produce strong vegetation volume scattering, which shows up more strongly in the HV channel (green). Over the Fen site, the signal is dominated by surface scattering, and therefore a good amount of both HH and VV is observed.

2) L-Band Twin Otter Data: Fig. 9 presents the maps of the calibrated L-band brightness temperatures acquired at a 40° incidence angle, in H and V polarizations (TB_H and TB_V) by the Twin Otter over the Kenaston site on 13 June. The two maps exhibit similar pattern in the variability of the brightness temperatures which results from soil moisture variability (Section IV-A1), topography (Fig. 2), and other surface conditions (Table I). Low values of brightness temperature values

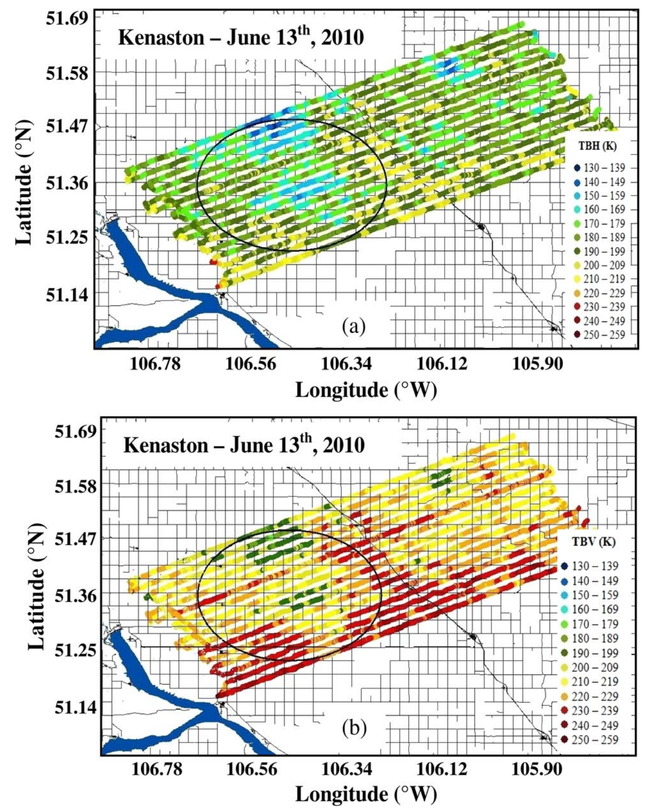

Fig. 9. Maps of L-band TB_H and TB_V measured by the Twin Otter over Kenaston site on 13 June, 2010. The circle of 31-km diameter is centered on the SMOS grid ID 147226 (51.35 N, 106.43 W).

are observed in the valley (falling in the delineated circle) while high values are measured in the Eastern part of the study area where high topography dominates (Fig. 2). Furthermore, a decreasing trend is observed in the brightness temperatures from south to north.

Fig. 10 shows that over the BERMS site, both TB_H and TB_V are affected by radio frequency interference (RFI) to different degrees. RFI will result in higher than expected brightness temperatures. In the eastern part of the BERMS site, the first three flight lines appear free of RFI. The remaining flight lines have varying degrees of RFI. Some brightness temperature values are very high, up to 9250 and 4400 K for the H and V polarizations, respectively. These values are far above the natural emission which is less than 300 K. Furthermore, Fig. 10 shows that the RFI is polarization dependent. In fact, TB_V is spatially less affected than TB_H. However, the later is more affected in terms of signal's magnitude.

The possible source of RFI we identified in the BERMS site is the use of communication antennas with a central bandwidth very close to the protected L-band (1.4–1.5 GHz). The flight lines with the highest RFI are within the corridor along which the antennas are transmitting. Some previous L-band airborne experiments conducted in the framework of SMOS Cal/Val activities have also suffered from RFI, and methods have been developed and applied for RFI detection and mitigation [30]–[32].

3) SMOS and AMSR-E: The SMOS brightness temperature (L1c product) and soil moisture (L2 product) data used in this paper correspond to 6 A.M. acquisitions. They were processed

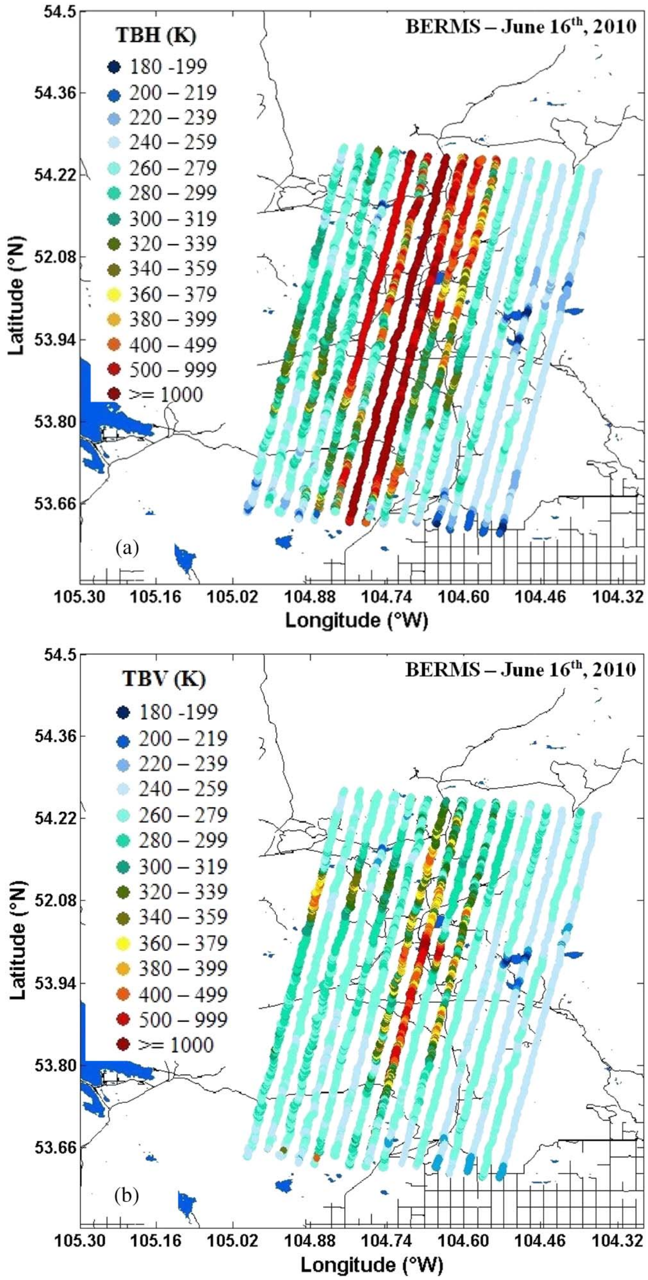

Fig. 10. Maps of TB_H and TB_V measured by the Twin Otter over BERMS site on 16 June, 2010.

with the prototypes 346 and 307, respectively. The AMSR-E soil moisture estimates used in this paper are from the National Snow and Ice Data Center (AMSR-E/NSIDC) [33]. They resulted from AMSR-E acquisitions at 1:30 P.M.

The primary focus of this paper is to present CanEx-SM10 experiment and the preliminary results on ground and remote sensing data. Therefore, no filtering was applied to SMOS data. A preliminary analysis of these SMOS data has been conducted to assess the angular variation, temporal evolution, and polarization dependency of the data with respect to differences in vegetation conditions (agricultural versus forested areas). SMOS data, shown in Figs. 11–13 for the Kenaston and BERMS sites, correspond, respectively, to the center grid IDs 147 226 (51.35 N, 106.43 W) and 139 552 (53.80 N, 104.70 W).

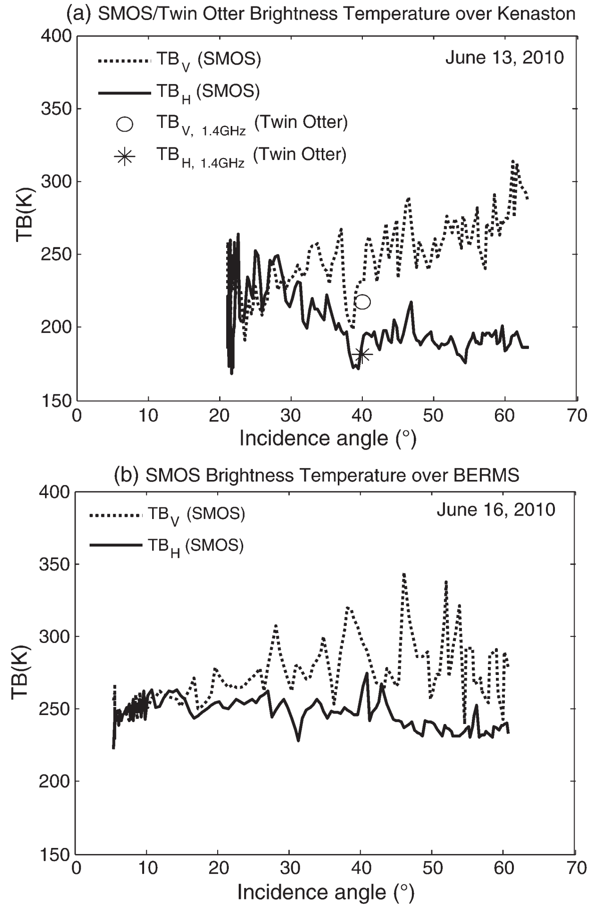

Fig. 11. Angular profiles of SMOS TB_H and TB_V measurements at 6 A.M. over (a) Kenaston on 13 June, 2010 and (b) BERMS on 16 June, 2010. Twin Otter airborne brightness temperatures are compared to SMOS data over Kenaston site. Airborne data over BERMS contaminated by RFI is not shown. (a) SMOS/Twin Otter brightness temperature over Kenaston; (b) SMOS brightness temperature over BERMS.

As observed with the Twin Otter's L-band airborne data, the SMOS brightness temperatures acquired over BERMS are more significantly impacted by RFI $(TB > 300\ K)$ relative to the Kenaston acquisitions. Similar to the study by Park *et al.* [34] conducted in North America, only low-level RFI contamination is observed in the SMOS brightness temperatures acquired over both sites (Fig. 11). The difference observed between the brightness temperatures of the Kenaston and BERMS sites is in accord with the theory [35] and previous results obtained from field experiments [36], [37]. Indeed, over Kenaston, the observed signals should be representative of bare wet soil conditions and thus have low values, while the higher brightness values over BERMS are a result of a high vegetation contribution and a low soil contribution due to the attenuation from the forest layer.

Angular variation: The angular profiles of SMOS brightness temperature (TB_H and TB_V) acquired on 13 June and on 16 June over, respectively, the Kenaston and BERMS sites are shown in Fig. 11. The Twin Otter data at 40° not corrupted by RFI, over Kenaston, are also presented in Fig. 11(a). These temperatures are average values calculated over the circle of 31-km diameter delineated in Fig. 9. This circle is centered on the aforementioned SMOS grid center # ID 147 226 (51.35 N,

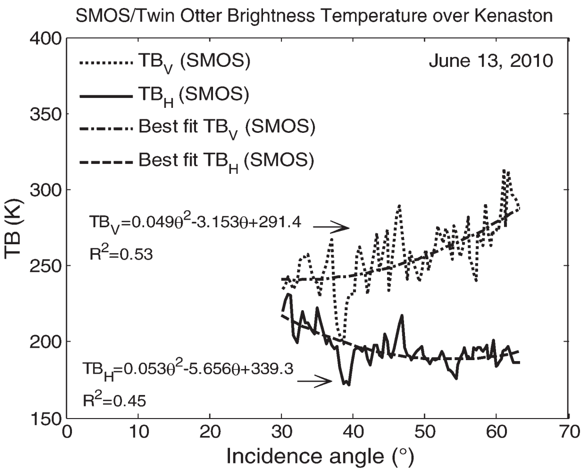

Fig. 12. Example of polynomial best fits obtained between the SMOS brightness temperatures (TBH, TBV) acquired at 6 A.M. over Kenaston on 13 June, 2010 and the incidence angles.

106.43 W) located in Kenaston. The observed angular behaviors over Kenaston and BERMS are typical of soil and vegetation layers, respectively [35], [38]. While the difference between TB_H and TB_V increases with the incidence angle over Kenaston (where bare soil conditions dominate), this difference is reduced over the BERMS forested site where a very weak angular dynamic is present. Good correspondence between SMOS and Twin Otter data can be observed over Kenaston on 13 June. Due to the impact of RFI on the Twin Otter acquisitions over BERMS (Fig. 10), no comparison is made between these data and SMOS measurements.

Temporal evolution: Due to the variability observed in SMOS brightness temperatures for both H and V polarizations (Fig. 11), functions were fitted to the angular profiles of TB_H and TB_V measurements. Fig. 12 shows examples of polynomial best fits obtained between SMOS TB_H and TB_V acquisitions on 13 June, 2010 over Kenaston. These functions were used to simulate SMOS data at 40° incidence angle for H and V polarizations in order to make a comparison with the temporal evolution of the L-band airborne brightness temperatures.

The temporal evolution of SMOS brightness temperatures (TB_H, TB_V) obtained at a 40° incidence angle from the best fit functions and that of the SMOS estimated soil moisture are provided in Fig. 13. Twin Otter data at 40° that was not corrupted by RFI over Kenaston are also presented. In addition, field measured soil moisture, precipitation [39] and AMSR-E/NSIDC soil moisture estimates [33] are also included in this figure. Fig. 13(a) shows that SMOS and the airborne brightness temperatures acquired over the Kenaston site exhibit similar temporal trends. However, in contrast to Fig. 11(a), there is a discrepancy between the SMOS data obtained from the best fits (Fig. 12) and the airborne measurements, with an evident bias difference which is present for all days of measurements, particularly in the V polarization (Fig. 11). Considering the range of variation of the root mean square error (RMSE) values of these best fit functions over the Kenaston site and the range of variation of the STD of the airborne data over an area of 31-km diameter of the Kenaston site (Table VII), this discrepancy can partially be explained.

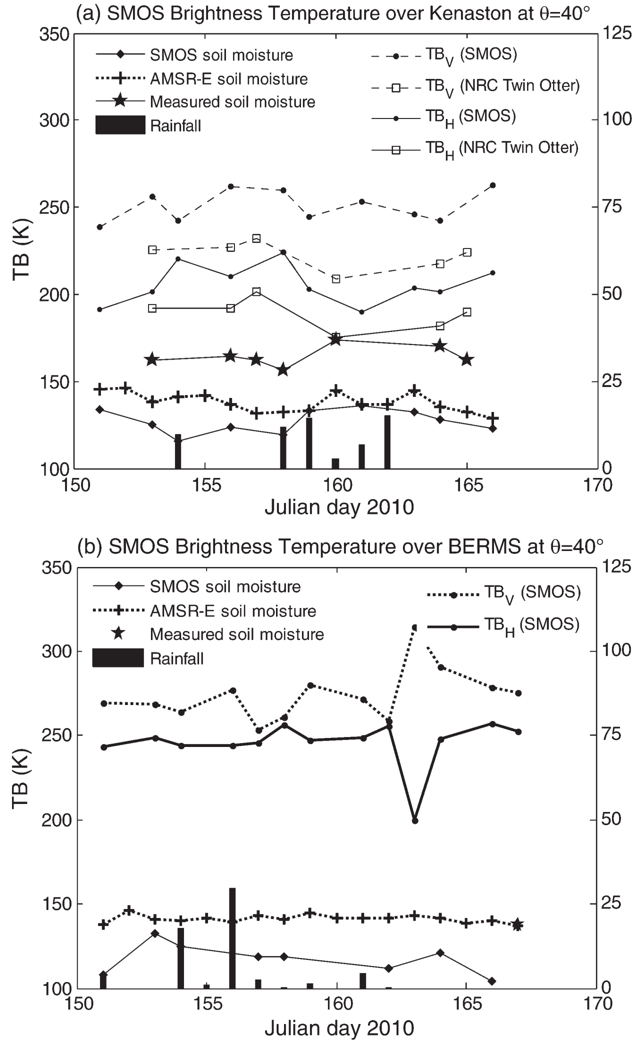

Fig. 13. Temporal evolution of SMOS brightness temperatures at 6 A.M. $(TB_H, TB_V$ obtained at 40° incidence angle from the best fit functions) and retrieved soil moisture from SMOS, together with field measured soil moisture, precipitation downloaded from Environment Canada database [39], and AMSR-E/NSIDC soil moisture estimated values at 1:30 P.M. [33]. (a) Over Kenaston with L-band airborne brightness temperatures in H and V polarizations, (b) over BERMS. (a) SMOS brightness temperature over Kenaston at $\theta = 40°$; (b) SMOS brightness temperature over BERMS at $\theta = 40°$.

TABLE VII
RANGE OF VARIATION OF THE ROOT MEAN SQUARE ERROR (RMSE) VALUES OF THE BEST FUNCTIONS FITTING THE SMOS ANGULAR PROFILES OVER THE KENASTON SITE AND THE STANDARD DEVIATION (STD) OF THE AIRBORNE DATA OVER AN AREA OF 31-km DIAMETER OF THE KENASTON SITE

	RMSE (K) of the best fit functions		**STD (K) of airborne data over an area of 31 km diameter**	
Polarization	H	V	H	V
Min	3.8	7.8	10.5	8.3
Max	29.5	35.4	15.2	13.1
Mean	7.3	15.3	12.1	9.8

The response in brightness temperature as a function of polarization is as expected. Indeed, depolarization of the signal occurs over the BERMS site where a more significant vegetation canopy is present (Figs. 11 and 13).

Fig. 13(a) shows more variation in SMOS TB_H than in TB_V measurements over Kenaston, which may be a result of the greater sensitivity of H polarization to soil conditions relative to

V polarization. While consistent temporal trends are observed between the soil moisture as measured throughout the CanEx-SM10 experiment, the airborne data, and SMOS TB_H, only a small agreement is observed with the trend in the SMOS brightness temperatures acquired in the V polarization. Indeed, the adverse weather conditions during the experiment reduced the number of soil moisture measurements, and these data gaps make it more difficult to compare the temporal trends in soil moisture measurements with that of the SMOS brightness temperatures.

Over BERMS [Fig. 13(b)], TB_H appears more stable than over Kenaston. This confirms the observation that over the BERMS forested site, the signal is less sensitive to variations in soil conditions relative to Kenaston. TB_H and TB_V measurements on Julian day 163 (12 June) were erroneous; indeed, TB_V is somewhat higher than natural emission ($TB_V > 300$ K) while TB_H falls to $\sim$200 K.

For the Kenaston and BERMS sites, the retrieval STD of SMOS soil moisture algorithm (which are the theoretical errors resulting from the cost function of the SMOS soil moisture algorithm; they do not correspond to the errors between the SMOS soil moisture estimations and the ground measurements of soil moisture) vary, respectively, from 12.10^{-4} to 66.10^{-4} m^3/m^3 and from 19.10^{-4} to 125.10^{-4} m^3/m^3. Since these values are very low, they are not plotted along the SMOS soil moisture estimations in Fig. 13.

To avoid a direct comparison between the *in situ* soil moisture and soil moisture estimated from the SMOS algorithm (L2 product), the *in situ* soil moisture measurements were computed at the SMOS resolution using the SMOS antenna weighting function [40]. No interpolation was applied before to *in situ* data collected over the entire study area. However, the SMOS antenna weighting function was applied to fields surrounding a SMOS grid center within an area of 123 km by 123 km covered by the antenna beam. As shown in Fig. 2, our soil moisture sampling points did not cover the whole area of 123 km by 123 km. They are distributed over an area of about 33 km $\times$ 71 km. Furthermore, the SMOS grids considered are agricultural or forested, not a mix of forest and agriculture. Therefore, the calculation of the weighted average soil moisture values did not take into account a fraction of forest versus nominal (low vegetation amount), because it does not apply. More details on the weighting process are available in [40].

Over both the Kenaston and BERMS sites, SMOS significantly underestimates soil moisture when compared to field measured moisture computed from the weighting function. Thus, the accuracy requirements (0.04 m3/m3) for the SMOS mission [5], [6] are not met with this data set based on the processing and analysis of the ground data we have conducted to date. Inadequate characterization of the vegetation contribution in the SMOS soil moisture estimation algorithm may offer one explanation. This problem is under consideration by many researchers, and eventual errors in the initial estimate of the vegetation optical depth should be corrected since the SMOS L2 algorithm is iterative. Furthermore, it should be noted that due to RFI or to imperfect multiangular trends (strong fluctuations) of the SMOS brightness temperatures, the retrieved values of SMOS soil moisture are not always based on all available angles. Therefore, some parts of the pixel may have been better covered than others. Over Kenaston, the soil moisture measurements and the estimates from SMOS (L2 products) followed a similar temporal trend, but with an absolute soil moisture offset of about 0.15 m3/m3. Considering the range of variation of the STD values [0.05–0.08 m3/m3] of the soil moisture measurements, SMOS and AMSR-E soil moisture estimates shown in Fig. 13(a) do not fall within the range of field values. Such an evaluation cannot be completed for BERMS, since only one day of field measurements is available. In Fig. 13, AMSR-E/NSIDC soil moisture estimates are much closer to the soil moisture measurements than the SMOS estimates. Recently, using soil moisture measurements from networks located in the U.S., Jackson [41] showed that despite its higher frequency AMSR-E performed similarly to SMOS.

V. CanEx-SM10 Data Base

A CanEx-SM10 database is under development. It will include all field and remote sensing data sets acquired during CanEx-SM10, with the exception of satellite SAR and optical data (due to potential licensing issues). Once all quality assurances have been made, the data set is expected to be released to the general public in June 2012 through the CanEx-SM10 web site [13].

VI. Conclusion

The paper presents an overview of the data set collected during the CanEx-SM10 experiment. This experiment took place from 31 May to 16 June 2010 over an agricultural site (Kenaston) and a boreal forest (BERMS) located in Saskatchewan, Canada. Each site covered an area of 33 km $\times$ 71 km which corresponds to about two SMOS pixels. Soils were uncharacteristically wet at the Kenaston site due to above-normal precipitation prior to and during the campaign. Field measured volumetric soil moisture ranged from 0.20 to 0.45 m^3/m^3 with significant field to field variability in moisture conditions. Summer and spring tillage created macro structure in some fields and thus soil roughness varied from field to field and roughness parameters (root mean square and correlation statistics) varied depending on the direction of measurement. As for the vegetation, the consistency of data was evaluated by examining the empirical relationships between the LAI and crop fractional cover over the Kenaston site, and between tree heights and the DBH over the BERMS site.

Over both the Kenaston and BERMS sites, both airborne and satellite microwave data were collected near the SMOS overpass times and coincident with ground-based measurements. Both the UAVSAR and the Twin Otter aircraft acquisitions at L-band captured the surface conditions observed during the experiment. The RFI observed in the SMOS and the L-band airborne radiometer data sets was characterized by strong spatial and temporal variability and polarization dependency.

The airborne and satellite data acquired, as well as the field measurements and data available from long-term soil moisture networks present at the sites, will support the validation of SMOS data and products and contribute to the prelaunch assessment of the proposed SMAP mission. SMOS is in its early operational phase (since June 2010) and the large data set collected during CanEx-SM10 can be used to correct SMOS soil moisture estimated values (L2 product). For subsequent validation and modeling studies, SMOS data should be filtered to remove artefacts due to RFI and other radiometric noises. Early analysis has determined that SMOS L2 products significantly underestimate soil moisture over both the Kenaston and BERMS sites. For these data, the accuracy requirements ($0.04\ \mathrm{m}^3/\mathrm{m}^3$) of the SMOS mission are not met. The AMSR-E/NSIDC soil moisture estimates more closely reflected the soil moisture conditions observed on the ground. Future work will focus on the development of improved soil moisture retrieval algorithms and disaggregation methods using the CanEx-SM10 data set.

ACKNOWLEDGMENT

CanEx-SM10 was a joint effort of Canadian and American research and academic institutions (Université de Sherbrooke/Centre d'applications et de recherches en télédétection, U of G, EC, Agriculture and Agri-Food Canada, USDA- Hydrology and Remote Sensing Lab, NASA, JPL of the California Institute of Technology, and University of Michigan). The authors would like to thank the funding agencies and all the participants in CanEx-SM10, the ESA for providing the SMOS data, the National Snow and Ice Data Cente for providing AMSR-E soil moisture data, the Centre d'Etudes Spatiales de la BIOSphère (Toulouse, France) for providing help with the SMOS data processing, and the two anonymous reviewers for their comments and suggestions to improve the quality of the paper.

REFERENCES

[1] M. Jung, M. Reichstein, P. Ciais, S. I. Seneviratne, J. Sheffield, M. L. Goulden, G. Bonan, A. Cescatti, J. Chen, R. de Jeu, A. J. Dolman, W. Eugster, D. Gerten, D. Gianelle, N. Gobron, J. Heinke, J. Kimball, B. E. Law, L. Montagnani, Q. Mu, B. Mueller, K. Oleson, D. Papale, A. D. Richardson, O. Roupsard, S. Running, E. Tomelleri, N. Viovy, U. Weber, C. Williams, E. Wood, S. Zaehle, and K. Zhang, *Recent Decline in the Global land Evapotranspiration Trend Due to Limited Moisture Supply*. New York: Macmillan, 2010.

[2] S. Bélair, L.-P. Crevier, J. Mailhot, B. Bilodeau, and Y. Delage, "Operational implementation of the ISBA land surface scheme in the Canadian regional weather forecast model. Part I: Warm season results," *J. Hydrometeorol.*, vol. 4, no. 2, pp. 352–370, Apr. 2003.

[3] R. D. Koster, M. J. Suarez, P. Liu, U. Jambor, A. Berg, M. Kistler, R. Reichle, M. Rodell, and J. S. Famiglietti, "Realistic initialization of land surface states: Impacts on subseasonal forecast skill," *J. Hydrometeorol.*, vol. 5, no. 6, pp. 1049–1063, Dec. 2004.

[4] A. A. Berg and K. Mulroy, "Streamflow predictability given macro-scale estimates of the initial soil moisture status," *Hydrol. Sci. J.*, vol. 51, pp. 642–654, 2006.

[5] Y. H. Kerr, P. Waldteufel, J.-P. Wigneron, J. Martinuzzi, J. Font, and M. Berger, "Soil moisture retrieval from space: The Soil Moisture and Ocean Salinity (SMOS) mission," *IEEE Trans. Geosci. Remote Sens.*, vol. 39, no. 8, pp. 1729–1735, Aug. 2001.

[6] H. M. J. P. Barré, B. Duesmann, and Y. H. Kerr, "SMOS: The mission and the system," *IEEE Trans. Geosci. Remote Sens.*, vol. 46, no. 3, pp. 587–593, Mar. 2008.

[7] D. Entekhabi, E. G. Njoku, P. E. O'Neill, K. H. Kellogg, W. T. Crow, W. N. Edelstein, J. K. Entin, S. D. Goodman, T. J. Jackson, J. Johnson, J. Kimball, J. R. Piepmeier, R. D. Koster, N. Martin, K. C. McDonald, M. Moghaddam, S. Moran, R. Reichle, J. C. Shi, M. W. Spencer, S. W. Thurman, L. Tsang, and J. Van Zyl, "The soil moisture active passive (SMAP) mission," *Proc. IEEE*, vol. 8, no. 5, pp. 704–716, May 2010.

[8] M. Vall-llossera, A. Camps, I. Corbella, F. Torres, N. Duffo, A. Monerris, R. Sabia, D. Selva, C. Antolín, E. López-Baeza, J. F. Ferrer, and K. Saleh, "SMOS REFLEX 2003: L-band emissivity characterization of vineyards," *IEEE Trans. Geosci. Remote Sens.*, vol. 43, no. 5, pp. 973–982, May 2005.

[9] P. de Rosnay, J. C. Calvet, Y. Kerr, J.-P. Wigneron, F. Lemaître, M. J. Escorihuela, J. M. Sabater, K. Saleh, J. Barrié, G. Bouhours, L. Coret, G. Cherel, G. Dedieu, R. Durbe, N. E. Fritz, F. Froissard, J. Hoedjes, A. Kruszewski, F. Lavenu, D. Suquia, and P. Waldteufel, "SMOSREX: A long term field campaign experiment for soil moisture and land surface processes remote sensing," *Remote Sens. Environ.*, vol. 102, no. 3/4, pp. 377–389, 2006.

[10] R. Panciera, J. P. Walker, J. D. Kalma, E. J. Kim, J. M. Hacker, O. Merlin, M. Berger, and N. Skou, "The NAFE'05/CoSMOS data set: Toward SMOS soil moisture retrieval, downscaling, and assimilation," *IEEE Trans. Geosci. Remote Sens.*, vol. 46, no. 3, pp. 736–745, Mar. 2008.

[11] M. Zribi, M. Pardé, J. Boutin, P. Fanise, D. Hauser, M. Dechambre, K. Kerr, M. Leduc-Leballeur, G. Reverdin, N. Skou, S. Søbjærg, C. Albergel, J.-C. Calvet, J.-P. Wigneron, E. Lopez-Baeza, A. Rius, and J. Tenerelli, "CAROLS: A new airborne L-band radiometer for ocean surface and land observations," *Sensors*, vol. 11, pp. 719–742, Jan. 2011. doi:10.3390/s110100719.

[12] [Online]. Available: http://earth.eo.esa.int/workshops/SVRT_Workshop/

[13] [Online]. Available: http://pages.usherbrooke.ca/canexsm10/

[14] S. Delwart, C. Bouzinac, P. Wursteisen, M. Berger, M. Drinkwater, M. Martín-Neira, and Y. H. Kerr, "SMOS validation and the COSMOS campaigns," *IEEE Trans. Geosci. Remote Sens.*, vol. 46, no. 3, pp. 695–704, Mar. 2008.

[15] [Online]. Available: http://www.geobase.ca/

[16] [Online]. Available: http://pages.usherbrooke.ca/canexsm10/Experimental_plan_CANEx-SM10.pdf

[17] I. Gherboudj, R. Magagi, K. Goïta, A. A. Berg, B. Toth, and A. Walker, "Validation of SMOS data over agricultural and boreal forest areas in Canada," *IEEE Trans. Geosci. Remote Sens.*, vol. 50, pt. 1, no. 5, pp. 1623–1635, May 2012.

[18] [Online]. Available: http://berms.ccrp.ec.gc.ca/Sites/e-sites.htm

[19] Steven Water Monitoring Syst. Inc., Portland, OR, Comprehensive Steven hydra Probe Users Manual, 2007, *92915*.

[20] C. Champagne, A. A. Berg, J. Belanger, H. McNairn, and R. deJeu, "Evaluation of soil moisture derived from passive microwave remote sensing over agricultural sites in Canada using ground-based soil moisture monitoring networks," *Int. J. Remote Sens.*, vol. 31, no. 14, pp. 3669–3690, Apr. 2010.

[21] M. Trudel, F. Charbonneau, F. Avendano, and R. Leconte, "Quick Profiler (QuiP): A friendly tool to extract roughness statistical parameters using a needle profiler," *Can. J. Remote Sens.*, vol. 36, no. 4, pp. 391–396, 2010.

[22] [Online]. Available: http://uavsar.jpl.nasa.gov/

[23] J. Famiglietti, D. Ryu, A. A. Berg, M. Rodell, and T. J. Jackson, "Field observations of soil moisture variability across scales," *Water Resour. Res.*, vol. 44, pp. W01 423-1–W01 423-16, 2008. doi:10.1029/2006WR005804.

[24] [Online]. Available: http://www.fluxnet.ornl.gov/fluxnet/sitesearch.cfm

[25] R. Magagi, M. Bernier, and C. H. Ung, "Quantitative analysis of RADARSAT SAR data over a sparse forest canopy," *IEEE Trans. Geosci. Remote Sens.*, vol. 40, no. 6, pp. 1301–1313, Jun. 2002.

[26] R. Rahmoune, A. D. Vecchia, P. Ferrazzoli, L. Guerriero, and F. Martin-Porqueras, "Refinements and tests of a microwave emission model for forests," in *Proc. Int. Geosci. Remote Sens. Symp.*, Cape Town, South-Africa, 2009, vol. II, pp. 278–281.

[27] C. G. Brown, Jr., K. Sarabandi, and L. E. Pierce, "Model-based estimation of forest canopy height in red and austrian pine stands using shuttle radar topography mission and ancillary data: A proof-of-concept study," *IEEE Trans. Geosci. Remote Sens.*, vol. 48, no. 3, pp. 1105–1118, Mar. 2010.

[28] A. D. Vecchia, P. Ferrazzoli, L. Guerriero, R. Rahmoune, S. Paloscia, S. Pettinato, and E. Santi, "Modeling the multifrequency emission of broadleaf forests and their components," *IEEE Trans. Geosci. Remote Sens.*, vol. 48, no. 1, pp. 260–272, Jan. 2010.

[29] I. Mladenova, private communication, 2011.

[30] N. Skou, S. Misra, J. Balling, S. Kristensen, and S. Søbjærg, "L-band RFI as experienced during airborne campaigns in preparation for SMOS," *IEEE Trans. Geosci. Remote Sens.*, vol. 48, pt. 2, no. 3, pp. 1398–1407, Mar. 2010.

[31] M. Pardé, M. Zribi, P. Fanise, and M. Dechambre, "Analysis of RFI issue using the CAROLS L-band experiment," *IEEE Trans. Geosci. Remote Sens.*, vol. 49, no. 3, pp. 1063–1070, Mar. 2011.

[32] E. Anterrieu, "On the detection and quantification of RFI in L1a signals provided by SMOS," *IEEE Trans. Geosci. Remote Sens.*, vol. 49, no. 10, pp. 3986–3992, Oct. 2011.

[33] E. G. Njoku, "Updated daily AMSR-E/Aqua daily L3 surface soil moisture, interpretive parameters, & QC EASE-Grids V002," National Snow and Ice Data Center, Boulder, CO, Jun. 1–16, 2010, Digital media.

[34] J. Park, J. T. Johnson, N. Majurec, N. Niamsuwan, J. R. Piepmeier, P. N. Mohammed, C. S. Ruf, S. Misra, S. H. Yueh, and S. J. Dinardo, "Airborne L-band radio frequency interference observations from the SMAPVEX08 campaign and associated flights," *IEEE Trans. Geosci. Remote Sens.*, vol. 49, no. 9, pp. 3359–3369, Sep. 2011.

[35] F. T. Ulaby, R. K. Moore, and A. K. Fung, *Microwave Remote Sensing*, vol. 3. Dedham, MA: Artech House, 1986.

[36] M. Guglielmetti, M. Schwank, C. Mätzler, C. Oberdörster, J. Vanderborght, and H. Flühler, "FOSMEX: Forest soil moisture experiments with microwave radiometry," *IEEE Trans. Geosci. Remote Sens.*, vol. 46, no. 3, pp. 727–735, Mar. 2008.

[37] J. P. Grant, A. A. Van de Griend, J.-P. Wigneron, K. Saleh, R. Panciera, and J. P. Walker, "On the influence of forest cover fraction on L-band soil moisture retrievals from heterogeneous pixels using multi-angular observations," *Remote Sens. Environ.*, vol. 114, no. 5, pp. 1026–1037, 2010.

[38] J. P. Grant, J.-P. Wigneron, A. A. Van de Griend, A. Kruszewsky, S. S. Søbjærg, and N. Skou, "A field experiment on microwave forest radiometry: L-band signal behaviour for varying conditions of surface wetness," *Remote Sens. Environ.*, vol. 109, no. 1, pp. 10–19, Jul. 2007.

[39] [Online]. Available: http://www.climat.meteo.gc.ca/

[40] ESA and ARRAY sytems computing Inc., Issue 3.4, 24/01/2011 "Algorithm theoretical based document (ATBD) for the SMOS Level 2 Soil Moisture Processor Development Continuation Project," prepared by CESBIO, IPSL-Service d'Aeronomie, INRAEPHYSE, Reading University, Tor Vergata University, Issue 3.4, 24/01/2011.

[41] T. J. Jackson, "Soil moisture validation with U.S. networks," presented at the Proc. SMOS VRT Workshop, Frascati, Italy, Nov. 29–30, 2010.

Ramata Magagi (M'08) received the B.S. degree in physics from the Université de Niamey, Niger, in 1991, and the Ph.D. degree in physics and chemistry of environment from the Institut National Polytechnique de Toulouse, Toulouse, France, in 1995.

From 1998 to 2000, she was a Postdoctoral Fellow with the Institut National de la Recherche Scientifique-Eau, Sainte-Foy, QC, Canada. From 2001 to 2002, she was a Research Associate in the Division of Engineering and Applied Sciences, at Harvard University, Cambridge, MA. Currently, she is an Associate Professor at Université de Sherbrooke, Sherbrooke, QC, Canada. Her research activities included microwave remote sensing of soil, snow, vegetation, and precipitation.

Aaron A. Berg received the B.Sc. and M.Sc. degrees in geography from the University of Lethbridge, Lethbridge, AB, Canada, in 1995 and 1997, respectively, the M.S. degree in geological sciences from the University of Texas at Austin, Austin, in 2001, and the Ph.D. degree in earth system science from the University of California, Irvine, in 2003.

Since 2003, he has been with the Department of Geography at the University of Guelph, Guelph, ON, Canada. Currently, he is an Associate Professor teaching in physical geography, hydrology, and remote sensing with research interests focused on the modeling and observation of soil moisture.

Kalifa Goïta (M'12) received the Ph.D. degree in remote sensing from the Université de Sherbrooke, QC, Canada, in 1995.

He is a Professor of geomatics with the Université de Sherbrooke and Head of the Department of Applied Geomatics. His research interest is in microwave remote sensing of land surface and satellite altimetry of continental waters.

Stephane Bélair is currently a Research Scientist in Environment Canada's Meteorological Research Division (MRD), Dorval, QC, where since 1997, has worked on improving the representation of physical processes in local, regional, and global numerical prediction weather systems. His work focuses on clouds, precipitation, boundary-layer turbulence, and land surface processes. He was the lead for MRD's global modeling group from 2001 to 2006 and has been since the lead for land surface modeling and assimilation.

Thomas J. Jackson (F'02) received the Ph.D. degree from the University of Maryland, College Park, in 1976.

He is a Research Hydrologist with the U.S. Department of Agriculture, Agricultural Research Service, Hydrology and Remote Sensing Laboratory, Beltsville, MD. His research involves the application and development of remote sensing technology in hydrology and agriculture, primarily microwave measurement of soil moisture. He is or has been a Member of the science and validation teams of the Aqua, ADEOS-II, Radarsat, Oceansat-1, Envisat, ALOS, SMOS, Aquarius, GCOM-W, and SMAP remote sensing satellites.

Dr. Jackson is a Fellow of the Society of Photo-Optical Instrumentation Engineers, the American Meteorological Society, and the American Geophysical Union. In 2003, he received the William T. Pecora Award (NASA and Department of Interior) for outstanding contributions toward understanding the Earth by means of remote sensing and the AGU Hydrologic Sciences Award for outstanding contributions to the science of hydrology. He received the IEEE Geoscience and Remote Sensing Society Distinguished Achievement Award in 2011.

Brenda Toth, photograph and biography not available at the time of publication.

Anne Walker received the B.A. and M.A. degrees in geography at Carleton University, Ottawa, ON, Canada, in 1984 and 1986, respectively.

In 1990, she was hired as a Physical Scientist with the Climate Research Division of Environment Canada. She has more than 25 years of experience conducting research on the application of passive microwave remote sensing data for investigating variability and change in cryospheric variables (snow cover, lake ice, and sea ice). Currently, she is a Research Manager within the Climate Research Division responsible for research programs focused on cold climate processes, their representation in climate models, and development of related observing techniques.

Heather McNairn received the Bachelor of Environmental Studies degree from the University of Waterloo, Waterloo, ON, in 1987, the M.Sc. degree in soil science from the University of Guelph, Guelph, ON, in 1992, and the Ph.D. degree in geography from Université Laval, Québec, QC, in 1999.

She has more than 20 years of experience in remote sensing research, working at the University of Guelph and the Canada Center for Remote Sensing prior to joining the Research Branch of Agriculture and Agri-Food Canada, Ottawa, ON, in 2003. She has led research projects to develop remote sensing methods for agriculture using multispectral, hyperspectral, and radar sensors. These projects have included the development of methods to map crops, soil tillage, crop residues, soil moisture, and crop biophysical properties.

Peggy E. O'Neill (M'85–SM'03) received the B.S. degree (*summa cum laude* with University Honors) in geography from Northern Illinois University, DeKalb, in 1976, the M.A. degree in geography from the University of California, Santa Barbara, in 1979, and has done postgraduate work in civil and environmental engineering through Cornell University, Ithaca, NY.

Since 1980, she has been employed as a Physical Scientist in the Hydrological Sciences Branch at NASA/Goddard Space Flight Center, Greenbelt, MD, where she conducts research in soil moisture retrieval and land surface hydrology, primarily through microwave remote sensing techniques. Currently, she is the Soil Moisture Active and Passive Deputy Project Scientist.

Mahta Moghaddam (S'86–M'87–SM'02–F'08) received the Ph.D. degree in electrical and computer engineering from the University of Illinois at Urbana-Champaign, Urbana, in 1991.

She is a Professor of electrical engineering at the University of Southern California, Los Angeles. She has introduced new approaches for quantitative interpretation of multichannel radar imagery based on analytical inverse scattering techniques applied to complex and random media. Her most recent research interests include the development of new radar instrument and measurement technologies for subsurface and subcanopy characterization, development of forward and inverse scattering techniques layered random media, and transforming concepts of radar remote sensing to near-field and medical imaging. She is a Member of the NASA advisory Council Earth Science Subcommittee, a Member of the Soil Moisture Active and Passive (SMAP) mission Science Definition Team, and the Chair of the SMAP Algorithms Working Group. She is the Principal Investigator of the AirMOSS NASA Earth Ventures mission.

Imen Gherboudj (A'12) received the Ph.D. degree in water science from the Institut National de la Recherche Scientifique, Quebec, QC, Canada, in 2008.

She was a Postdoctoral Researcher with the Centre d'Application et de Recherche en Télédétection, Université de Sherbrooke, Sherbrooke, QC, Canada. Currently, she is a Postdoctoral Researcher with the Earth Observation and Environmental Remote Sensing Laboratory of Masdar Institute, Abu-Dhabi, United Arab Emirates. Her research interests include the retrieval of the physical parameters of soil from active and passive microwave data.

Andreas Colliander (S'04–A'06–M'07–SM'08) received the M.Sc. (Tech.), Lic.Sc. (Tech.), and D.Sc. (Tech.) degrees from the Helsinki University of Technology (TKK; now Aalto University), Espoo, Finland, in 2002, 2005, and 2007, respectively.

From 2001 to 2007, he was with the Laboratory of Space Technology, TKK, where he was a Research Scientist and a Project Manager. From 2007 to 2008, he was a Postdoctoral Research Fellow with the European Space Research and Technology Center, ESA, Noordwijk, The Netherlands. Currently, he is a Research Scientist with the Jet Propulsion Laboratory, California Institute of Technology, Pasadena, where he is a Member of the Science Algorithm Development Team for the Soil Moisture Active and Passive mission.

Since 2009, he has been serving as a Cochair of the Microwave Radiometry Working Group of the Instrumentation and Future Technologies Technical Committee of the Geoscience and Remote Sensing Society of IEEE.

Michael H. Cosh received the B.A. degree in engineering, with minors in math and physics, from Saint Francis College, Loretto, PA, in 1995, the B.S. degree (*magna cum laude*, with honors) in civil and environmental engineering from The Pennsylvania State University, University Park, in 1996, and the M.S. degree in hydraulics and hydrology and the Ph.D. degree in environmental fluid mechanics and hydrology from the School of Civil and Environmental Engineering, Cornell University, Ithaca, NY, in 1998 and 2002, respectively.

He is a Research Hydrologist with the U.S. Department of Agriculture, Agricultural Research Service, Hydrology and Remote Sensing Laboratory, Beltsville, MD. His research involves the scaling of *in situ* ground data to remote sensing scales, spatial variability assessment of soil moisture, and developing methods to establish long-term validation sites for remote sensing platforms, including the use of temporal and spatial stability.

Mariko Burgin (S'09) received the M.S. degree in electrical engineering and information technology from the Eidgenössische Technische Hochschule Zurich (Swiss Federal Institute of Technology), Zurich, Switzerland, in 2008. Currently, she is working toward the Ph.D. degree in the Radiation Laboratory of the Department of Electrical Engineering and Computer Science, University of Michigan, Ann Arbor.

Her research interests include forward and inverse modeling of electromagnetic scattering from vegetated areas with special interest in forests, radar systems, and retrieval and radar measurements of vegetation and ground variables.

Joshua B. Fisher received the B.S. degree in environmental sciences and the Ph.D. degree in environmental science, policy, and management from the University of California, Berkeley, in 2001 and 2006, respectively.

He did his postdoctoral work at the University of Oxford, Oxford, U.K., then joined NASA's Jet Propulsion Laboratory, Pasadena, CA, in 2010. He has worked on ecosystem modeling for over 10 years, developed new models of hydrological and nutrient cycling, and conducted large-scale field campaigns to gather data to parameterize and test models. His work bridges modeling and field work, while integrating a wide range of measurement techniques such as eddy covariance and remote sensing.

Seung-Bum Kim received the B.S. degree in electrical engineering from the Korea Advanced Institute of Science and Technology (KAIST), Daejeon, Korea, in 1992, and the M.S. and Ph.D. degrees in remote sensing from the University College London, London, U.K., in 1993 and 1998, respectively.

He worked on spaceborne photogrammetry to generate land topography with the SPOT images and microwave radiometry with the AMSR-E data in KAIST until 2003 as a part of the national service. He conducted ocean science research of the mixed layer dynamics in the Jet Propulsion Laboratory (JPL) until 2006. He then became a Scientist at Remote Sensing Systems, California, studying the L-band radiometry for the Aquarius salinity observations. In 2009, he joined JPL. His current research includes microwave modeling, soil moisture retrieval with the radar data from the Soil Moisture Active Passive mission, and salinity retrieval with the Aquarius data. He received a graduate scholarship from KAIST and paper awards from U.K. and Korean remote sensing societies.

Iliana Mladenova (S'08–M'09) received the M.S. degree in hydrology and ecohydrology, with an emphasis in remote sensing, from the Vrije Universiteit, Amsterdam, The Netherlands, in 2006, and the Ph.D. degree in the same area from the University of South Carolina, Columbia, in 2009.

Between fall 2004 and spring 2006, she was with the Hydrology and Remote Sensing Laboratory, U.S. Department of Agriculture, Beltsville, MD, and in 2008, she spent three months with the Department of Civil and Environmental Engineering, Melbourne, Australia, focusing on studies in support of soil moisture algorithm development and validation, and downscaling issues. Currently, she is a Physical Research Scientist with the Hydrology and Remote Sensing Laboratory. She has an extensive experience in large-scale satellite and aircraft remote sensing validation experiments in support of NASA's AMSR-E and ESA's SMOS missions. Her research interests include microwave remote sensing of soil moisture, data assimilation, and remote sensing application in hydrology and agriculture.

Dr. Mladenova is a member of the IEEE Geoscience and Remote Sensing Society and the American Geophysical Union.

Najib Djamaï received the Engineering degree in hydrometeorology from Ecole Nationale d'Ingénieurs de Tunis, Tunis, Tunisia, in 2008, and the M.Sc. degree in geomatics from Université Laval, Quebec, QC, in 2010. Currently, he is working toward the Ph.D. degree at Université de Sherbrooke, Sherbrooke, QC.

His research focuses on downscaling of coarse resolution SMOS soil moisture product.

Louis-Philippe B. Rousseau, photograph and biography not available at the time of publication.

Jon Belanger received the B.A. degree in geography from the University of Guelph, Guelph, ON, Canada.

After moving on to a M.Sc.degree in geography at the University of Guelph, he was transferred to a Ph.D. program. His research focuses on upscaling and downscaling of soil moisture field for the validation of remotely sensed soil moisture products. He is also accoladed by the University of Guelph for his dedication to service and volunteerism.

Jiali Shang (M'12), photograph and biography not available at the time of publication.

Amine Merzouki received the B.Sc. degree in physics from Cadi Ayyad University, Marrakech, Morocco, in 1996, the M.Sc. degree in radiation physics from Hassan II-Mohamedia University, Casablanca, Morocco, in 1997, and the Ph.D. degree in remote sensing from University of Ottawa, Ottawa, ON, Canada, in 2007.

From 2002 to 2007, he worked in collaboration with the Canada Center of Remote Sensing where he contributed to the development of methods to model the spatial variability of soil moisture using synthetic aperture radar (SAR) data. In 2007, he joined the Faculty of Forestry and Environmental Management at University of New Brunswick, Fredericton, NB, Canada, as a Postdoctoral Fellow where he worked on Fire Weather Index codes mapping for vegetation moisture monitoring over Canadian grasslands ecosystems using optical, thermal infrared, and polarimetric SAR image data. In 2008, he joined the Research Branch of Agriculture and Agri-Food Canada, Ottawa, ON, where he has been leading research activities related to the development of polarimetric SAR applications to support the agricultural sector.